NASA Technical Memorandum 86741

Modified U.S. Army U-8F Ground Vibration Test

Michael W. Kehoe

August 1986

National Aeronautics and
Space Administration

NASA Technical Memorandum 86741

Modified U.S. Army U-8F Ground Vibration Test

Michael W. Kehoe
Ames Research Center, Dryden Flight Research Facility, Edwards, California

1986

National Aeronautics and
Space Administration
Ames Research Center
Dryden Flight Research Facility
Edwards, California 93523-5000

SUMMARY

The Dryden Flight Research Facility of NASA Ames Research Center conducted a ground vibration test on a modified U.S. Army U-8F airplane. Modifications included new engines, propellers, and engine-mount truss assemblies. The ground vibration test was conducted using sine dwell, single-point random, and impact excitations. The test was performed to determine modal frequencies, mode shapes, and structural damping coefficients of the airframe and propeller with full and empty fuel tanks. The data presented include frequency response plots, rigid-body and structural modal frequencies, and mode shapes.

INTRODUCTION

The U-8F is a twin-engine light aircraft manufactured by the Beech Aircraft Corporation. The U-8F is the U.S. Army designation of the Beechcraft Queen Air models 65 and A65. The model 65 airplane (fig. 1) is powered by two 340-hp six-cylinder horizontally opposed supercharged engines. Hartzell three-blade, fully feathering, constant-speed propellers are used with these engines. Each wing has a fuel capacity of 90 U.S. gal. Compared with the model 65, the model A65 has a swept vertical tail surface and an increased wing fuel capacity of 17 gal in each wing.

Excalibur Aviation Company modified the Queen Air A65 by replacing the engines with larger nonsupercharged 400-hp eight-cylinder horizontally opposed engines, by installing a new engine-mount truss assembly and a new three-blade propeller. A supplemental type certificate for the Queen Air A65 was obtained from the Federal Aviation Administration for this modification. There have been no reports of any problems with the modified Queen Air A65.

The U.S. Army U-8F was also modified similar to the commercial Queen Air A65 airplanes. The modified U-8F airplanes have experienced a wing vibration in flight. The amplitude of the vibration varies with the propeller rpm. The pilots have reported seeing the propeller blades bend in flight. The effect of wing fuel on the vibration is not known at this time.

At the request of the U.S. Army, a ground vibration test (GVT) was conducted on a modified U-8F airplane (model 65) at the Dryden Flight Research Facility of NASA Ames Research Center (Ames-Dryden) during the week of March 18, 1985. The objectives of the test were

1. To measure and record the frequencies for aircraft structural modes below 140 Hz.

2. To measure wing and engine nacelle mode shapes.

3. To observe any unusual vibratory motion of the structure.

VEHICLE CONFIGURATION

The GVT was conducted in the Flight Loads Research Facility at Ames-Dryden. The overall test setup is shown in figure 2. The vehicle used for this test was a

modified U.S. Army U-8F, serial 0-05390. This vehicle was similar to a Queen Air model 65. The aircraft was on its landing gear during the test. The landing gear struts were deflated. The tires were deflated to one-half of the normal pressure to provide a soft support. The control yoke gust lock was installed in the yoke to lock the ailerons and elevators in a neutral position. The rudder control surface was not locked in a neutral position. The top fiberglass fairing on each engine was removed in order to gain direct access to the engine for mounting the accelerometers. These fairings remained off during the test.

The aircraft fuel loadings for the test were full fuel tanks and empty fuel tanks. As a safety measure, the fuel tank vent lines were connected together by hoses and routed outside the hangar.

The right outboard flaps had a significant amount of free play. To ensure proper structural response, the outboard flaps on each wing were preloaded with 20.0 lb of lead shot suspended by a 3/8-in diameter bungee cord.

TEST EQUIPMENT

The GVT was conducted using sine dwell, single-point random, and impact excitation techniques. Some excitation equipment was common to these methods, while additional equipment was unique to each method.

Sine Dwell Equipment

The GVT equipment was housed in two portable consoles, one of which is shown in figure 3. The system was capable of acquiring, filtering, displaying, and recording six channels of accelerometer data. Electrodynamic shakers with current feedback and individual gain and phase controls were used to input a sinusoidal forcing function to the structure. Each shaker was attached to the aircraft by means of a telescoping thrust rod, a force link, and a mechanical fuse (fig. 4). The fuse was attached to a locking ball nut joint that was mounted directly to the structure by a threaded stud.

Piezoelectric accelerometers were attached to the aircraft to measure the response of the structure. The signal was amplified by a remote preamplifier and by a signal conditioning amplifier. The signal was then routed through tracking filters with a 2.00-Hz bandwidth. At this point, a patch panel was utilized to pass the output signal to several display and recording devices. These devices included two four-channel amplitude-time (X-t) oscilloscopes, a two-channel X-Y oscilloscope, three two-channel X-Y plotters, an eight-channel stripchart recorder, two digital rms voltmeters, and a coincident-quadrature analyzer.

Single-Point Random Equipment

The minicomputer-based structural analysis system used for the GVT was housed in one portable console (fig. 5). The system was capable of acquiring, filtering, displaying, and recording eight channels of data (one input and seven responses).

The system operates by exciting the airplane through one electrodynamic shaker with either a sinusoidal or a random forcing function and then analyzing the resultant vehicle response.

Impact Excitation Equipment

The single-point random equipment was used for impact excitation. An instrumented hammer was used in place of the electrodynamic shaker. The hammer was equipped with soft and hard heads to excite low and high frequencies, respectively. A soft head was used for this test. The total weight of the hammer was 0.5 lb.

TEST PROCEDURES

Sine Dwell Excitation

Multishaker techniques were used to excite the airplane rigid body and elastic modes that were not measured with the single-point random technique. Two vertical shakers were attached to the wingtips at the forward spar, and two vertical shakers were mounted on each engine at the propeller spinner.

Frequency sweeps. — The frequency sweeps were conducted from 2.00 to 140.00 Hz. A logarithmic sweep rate of 0.37 decade/min was used. Accelerometers were placed at several locations and in various orientations. The frequency response plots of these accelerometers were recorded on the X-Y plotters. These plots indicated frequencies of significant structural response.

Structural mode measurements. — After the frequency sweeps were completed, selected aircraft structural modes were fine-tuned using a coincident-quadrature analyzer. Each mode was tuned by minimizing the coincident component and maximizing the quadrature component of the signal. Time history traces of acceleration as a function of time were also used to verify phasing between the left and right sides of the airplane. Another check on the purity of the mode was to terminate electrical power to the shaker and observe the decay of the oscillations for beats. The absence of beats in the decay trace indicated that a mode was properly tuned.

Most of the accelerometer locations on the airplane that were used for measuring structural modes are shown in figure 6. (Points not shown are 123 to 125 and 302 to 303 that mirror points 223 to 225 and 402 to 403, respectively.) Once a mode was tuned, a modal survey was performed with the roving accelerometers. The point on the structure with the largest amplitude was selected as the reference point. The reference was used to normalize all other accelerometer response values and to determine phase relationships with roving accelerometers. Each roving accelerometer was placed at the reference point before a survey to compare amplitude readings. The accelerometer amplifier gains were adjusted as necessary to ensure uniform readings.

Single-Point Random Excitation

The single-point random excitation procedure and analysis are described in Leppert, et al., 1976, and Mirimand, et al., 1976. The system first generated a

random forcing function of a bandwidth and amplitude specified by the user. After the forcing spectrum was generated, the forcing function time history was recorded on a tape recorder. The signal was then played back through the electrodynamic shaker attached to the airplane.

Data were acquired with the structural analysis system at each of the locations shown in figure 6. Six accelerometer signals and the reference input force were input into the analyzer. Transfer and coherence functions were then calculated. The coherence function was used as a measurement of the quality of the data before storage on the system disk. The 140.00-Hz bandwidth was divided into smaller bandwidths of 0 to 50.00 Hz and 50.00 to 140.00 Hz. The 0- to 50.00-Hz data were sampled at 128 samples/sec using a data block size of 1024 samples (8 sec required to fill the block). The 50.00- to 140.00-Hz data were sampled at 384.24 samples/sec using a data block size of 1024 samples (2.67 sec required to fill the block). The total number of averages used to calculate each transfer function in each bandwidth was 50. A Hanning window (Bendat and Piersol, 1980) was used to reduce leakage errors.

When data acquisition was completed for the entire airplane, the frequency, damping, amplitude, and phase were estimated for each mode by fitting a multiple degree-of-freedom curve to a selected transfer function that exhibited a good response for the structural modes of interest. The estimated modal parameters, particularly phase, for each mode were examined to determine if the curve fit was acceptable. It was necessary to examine several different transfer functions to ensure a good curve fit for all structural modes.

After a good fit was obtained to estimate the modal parameters (frequency, damping, amplitude, and phase), the modal coefficients for each mode shape were calculated at all points by using the amplitude and phase of the measured response at the selected resonance frequency. Animated mode shapes were then displayed to identify each mode.

Impact Excitation

Each propeller blade was excited with an instrumented hammer at 12 locations as shown in figure 7. A single-axis piezoelectric accelerometer was attached to the tip of one blade to measure the response.

Data were acquired and analyzed for each impact location with the equipment and analysis method described in the test procedure for single-point random excitation. A bandwidth of 0 to 250.00 Hz was investigated for the propeller. The data were sampled at 512 samples/sec using a data block size of 1024 samples (2 sec required to fill the block). Five averages were used in each transfer function calculation.

RESULTS AND DISCUSSION

Frequency Sweeps

Multishaker frequency sweeps were performed with shakers connected at the wingtips and at the engines. Symmetric and antisymmetric sweeps were performed to identify approximate frequencies of structural modes. These sweeps were performed

on the airplane with both full and empty fuel tanks. The data are presented in the appendix.

Propeller Modal Frequencies

Six propeller modes were identified in the frequency range of 0 to 250.00 Hz. The frequency, damping, and phase are listed in table 1. The mode shapes are shown in figure 8. The 35.56-Hz mode was the first blade bending mode. The mode shape revealed very little motion on one of the blades. The second and third modes were second blade bending modes with a phasing difference between the three blades. The shape of the fourth mode, at 162.87 Hz, revealed third blade bending on one blade and second blade bending on the other two blades. The fifth and sixth modes were third blade bending with a phasing difference between the three blades.

Full Fuel Tank Modal Frequencies

The rigid body and the structural modes identified within a bandwidth of 50.00 Hz are listed in table 2. The measured mode shapes are shown in figures 9 to 19. The symmetric engine pitch mode shape was not completely measured because of time constraints. A partial survey was conducted to ensure that the symmetric pitch mode was excited. The wing torsion mode shape was shown to have greater amplitude on the left wing than on the right. This was caused by single-shaker excitation with the airplane resting on its landing gear.

The structural modes identified within a 50.00- to 140.00-Hz bandwidth were primarily control surface modes. Table 3 lists the frequency, damping, and phase values for each mode. Because the frequency sweeps indicated a difference between right and left control surfaces, each wing was excited and surveyed individually. The mode shape plots for the left wing (fig. 20) and the right wing (fig. 21) illustrate this. The difference between each wing was probably the result of the different amount of free play in each control surface. In particular, the right outboard flap had a large amount of free play. The left and right outboard flaps were preloaded with 20.0 lb of lead shot suspended from bungee cord to improve their response.

Empty Fuel Tank Modal Frequencies

The rigid body and structural modes identified for the airplane with no fuel are listed in table 4. The measured mode shapes are shown in figures 22 to 29. The left-wing mode shape amplitude was greater than that for the right wing for some modes because of single-shaker excitation with the airplane resting on its landing gear.

The full fuel tank configuration data indicated that the structural modes above 50.00 Hz were not excited with a single wingtip shaker. Hence, the bandwidth was not increased to 140.00 Hz for the empty fuel tank configuration. Only panel and control surface bending modes were excited above 50.00 Hz.

Modal Data Comparison

Data were obtained from the Beech Aircraft Corporation for the Queen Air model 65-80 airplane. The model 65-80 differs from the model 65 and A65 in that it has more powerful six-cylinder engines. Structurally, it is the same as the model A65 airplane. Its fuel capacity is the same as the model 65 and U-8F airplanes. A comparison of the U-8F data to the model 65-80 data is given in table 5. The largest differences in modal frequencies are for the antisymmetric engine pitch and wing bending modes. Data were not available for the symmetric engine pitch mode for the model 65-80 airplane. In general, the limited modal data comparison indicated that the U-8F is fairly similar to the unmodified model 65-80 airplane. The engine pitch modal frequencies were expected to be different because of the differences in engine weight and the engine-mount truss assembly of the modified U-8F airplane.

No data were available for the propeller of an unmodified commercial Queen Air aircraft. As a result, no direct comparison can be made for the U-8F propeller. It is interesting to note, however, that the 35.56-Hz propeller bending mode is excited by shaking at the wingtip.

CONCLUSIONS AND RECOMMENDATIONS

A ground vibration test was conducted on a modified U.S. Army U-8F airplane. The modification included replacing the engines with larger, more powerful engines, installing a new propeller, and installing a new engine-mount truss assembly. This modification is similiar to the one performed on the commercial Queen Air A65 airplane. The U-8F aircraft have experienced wingtip vibrations in flight whereas none have been reported for the Queen Air A65 aircraft. The amplitude of the vibrations was sensitive to propeller rpm.

Rigid body modes and structural modes were identified with the airplane empty and full of fuel. Mode shape data were taken for these two fuel configurations.

A comparison of modal data obtained from the ground vibration test and modal data for a Queen Air model 65-80 indicated that only the engine pitch and antisymmetric wing bending modal frequencies were different. A change in the engine pitch frequencies was expected because of the differences in engine weight and the engine-mount truss assembly for the modified airplane. Modal data were not available for the unmodified commercial Queen Air propeller to compare with the U-8F propeller. Because the modified U-8F structural modes were not significantly changed from the unmodified Queen Air, it appeared that the U-8F propeller may have been the potential source of the vibrations experienced in flight.

Ames Research Center
Dryden Flight Research Facility
National Aeronautics and Space Administration
Edwards, California, May 20, 1985

APPENDIX — FREQUENCY SWEEP PLOTS

This appendix contains the frequency sweep data obtained during the test. Table 6 summarizes the sweeps for the full fuel loading (figs. 30 to 52), and table 7 summarizes the sweeps for the empty fuel tank configuration (figs. 53 to 76). The 60.00-Hz mode that appears on some of the plots is not a structural mode but was caused by a 60-cycle ground loop in the GVT equipment. All frequency sweeps were conducted in the vertical direction.

REFERENCES

Bendat, Julius S.; and Piersol, Allan G.: Engineering Applications of Correlation and Spectral Analysis. John Wiley and Sons, Inc., New York, N.Y., 1980.

Leppert, E.L.; Lee, S.H.; Day, F.D.; Chapman, P.C.; and Wada, B.K.: Comparison of Modal Test Results: Multipoint Sine Versus Single-Point Random. SAE-760879, 1976.

Mirimand, N.; Billaud, J.F.; Leleux, F.; and Kreneuez, J.P.: Identification of Structural Modal Parameters by Dynamic Tests at a Single Point. Shock and Vibration Bull., vol. 46, part 5, 1976, pp. 197-212.

TABLE 1. — U-8F PROPELLER GROUND VIBRATION TEST, 0- to 250.00-HZ BANDWIDTH (fig. 8)

Frequency, Hz	Damping, $\bar{g}$	Force acceleration phase, deg
35.56	0.034	91
104.56	0.036	107
121.70	0.035	91
162.87	0.056	91
206.32	0.052	100
226.72	0.027	94

TABLE 2. — U-8F GROUND VIBRATION TEST (FULL FUEL TANKS), 3.00- to 50.00-HZ BANDWIDTH

Mode	Frequency, Hz	Damping, $\bar{g}$	Force acceleration phase, deg	Mode shape fig.
Wing				
First symmetric bending	6.86	0.038	90	12
Second symmetric bending	19.14	0.056	90	17
First antisymmetric bending	14.98	0.089	93	15
Torsion	34.30	0.058	-86	18
Aileron bending	41.18	0.072	-91	19
Engine				
Symmetric pitch	9.33	0.065	--[a]	--[b]
Antisymmetric pitch	6.76	0.034	--[a]	11
Symmetric lateral	8.03	0.060	87	13
Fuselage				
Torsion	10.19	0.073	-88	14
Tail assembly				
Symmetric horizontal stabilizer bending	15.99	0.033	97	16
Rigid body				
Roll	3.17	0.069	91	9
Pitch	4.17	0.106	-91	10

[a]Not applicable, sine dwell.

[b]Not applicable.

TABLE 3. — U-8F GROUND VIBRATION TEST (FULL FUEL TANKS), 50.00- to 140.00-HZ BANDWIDTH

Mode	Frequency, Hz	Damping, $\bar{g}$	Force acceleration phase, deg	Mode shape fig.
Left wing				
Aileron bending	65.62	0.064	95	20
Outboard flap bending	89.57	0.046	-95	20
Outboard flap bending	107.09	0.008	92	20
Outboard flap bending	110.06	0.012	88	20
Inboard flap bending	120.56	0.006	87	20
Outboard flap bending	132.12	0.014	85	20
Aileron bending	143.32	0.018	-81	20
Right wing				
Inboard flap bending	67.99	0.067	85	21
Inboard flap bending	84.54	0.041	89	21
Inboard flap bending	111.93	0.017	-88	21
Outboard flap bending	121.80	0.031	103	21
Aileron bending	123.21	0.006	-88	21
Inboard bending	125.17	0.011	106	21
Aileron bending	137.86	0.024	-95	21

TABLE 4. — U-8F GROUND VIBRATION TEST (EMPTY FUEL TANKS), 3.00- to 50.00-HZ BANDWIDTH

Mode	Frequency, Hz	Damping, $\bar{g}$	Force acceleration phase, deg	Mode shape fig.
Wing				
First symmetric bending	8.03	0.037	83	23
Second symmetric bending	24.64	0.078	-83	28
First antisymmetric bending	16.25	0.076	88	27
Torsion	38.02	0.107	82	29
Engine				
Symmetric pitch	9.47	0.062	--[a]	24
Antisymmetric pitch	7.02	0.057	92	22
Fuselage				
Torsion	10.56	0.036	-89	25
Tail assembly				
Symmetric horizontal stabilizer bending	15.88	0.038	95	26
Rigid body				
Roll	3.21	0.122	--[a]	--[b]
Pitch	3.54	0.061	--[a]	--[b]
Plunge	3.07	0.123	--[a]	--[b]

[a]Not applicable, sine dwell.

[b]Not applicable.

TABLE 5. — MODAL DATA COMPARISON
(FULL FUEL TANKS)

Mode	Aircraft model frequency, Hz	
	U-8F	65-80
Wing		
First symmetric bending	6.86	6.8
Second symmetric bending	19.14	19.2
First antisymmetric bending	14.98	15.8
Wing torsion	34.30	
Engine		
Symmetric pitch	9.33	
Antisymmetric pitch	6.76	7.6
Symmetric lateral	8.03	
Fuselage		
First vertical bending		27.5
First lateral bending		17.2
Torsion	10.19	10.0
Tail assembly		
Fin bending		14.5
Symmetric horizontal stabilizer bending	15.99	16.3

TABLE 6. — FREQUENCY SWEEP DATA
(FULL FUEL TANKS)

(a) Engine shakers

Figure	Force, lb	Excitation	Response location
30	10	Symmetric	101, 201
31	10	Symmetric	118, 218
32	10	Symmetric	306, 406
33	10	Antisymmetric	101, 201
34	10	Antisymmetric	118, 218
35	5	Antisymmetric	306, 406

(b) Wingtip shakers

Figure	Force, lb	Excitation	Response location
36	5	Symmetric	101, 201
37	5	Symmetric	118, 218
38	5	Symmetric	118, 218[a]
39	5	Symmetric	306, 406
40	5	Symmetric	110, 210
41	5	Symmetric	110, 210[b]
42	5	Symmetric	125, 225
43	5	Symmetric	103, 203
44	5	Symmetric	103, 203[b]
45	5	Antisymmetric	101, 201
46	5	Antisymmetric	118, 218
47	5	Antisymmetric	118, 218[a]
48	5	Antisymmetric	306, 406
49	5	Antisymmetric	125, 225
50	5	Antisymmetric	110, 210[b]
51	5	Antisymmetric	103
52	5	Antisymmetric	103, 203[b]

[a]Lateral

[b]10-lb preload

TABLE 7. — FREQUENCY SWEEP DATA
(EMPTY FUEL TANKS)

(a) Engine shakers

Figure	Force, lb	Excitation	Response location
53	10	Symmetric	101, 201
54	10	Symmetric	118, 218
55	10	Symmetric	306, 406
56	10	Antisymmetric	101, 201
57	10	Antisymmetric	118, 218
58	10	Antisymmetric	306, 406

(b) Wingtip shakers

Figure	Force, lb	Excitation	Response location
59	5	Symmetric	101, 201
60	5	Symmetric	118, 218
61	5	Symmetric	118, 218[a]
62	5	Symmetric	306, 406
63	5	Symmetric	125, 225
64	5	Symmetric	110, 210
65	5	Symmetric	110, 210[b]
66	5	Symmetric	103, 203
67	5	Symmetric	Propeller tip
68	5	Antisymmetric	101, 201
69	5	Antisymmetric	118, 218
70	5	Antisymmetric	118, 218[a]
71	5	Antisymmetric	306, 406
72	5	Antisymmetric	502, 503
73	5	Antisymmetric	125, 225
74	5	Antisymmetric	110, 210
75	5	Antisymmetric	110, 210[b]
76	5	Antisymmetric	103, 203

[a]Lateral

[b]10-lb preload

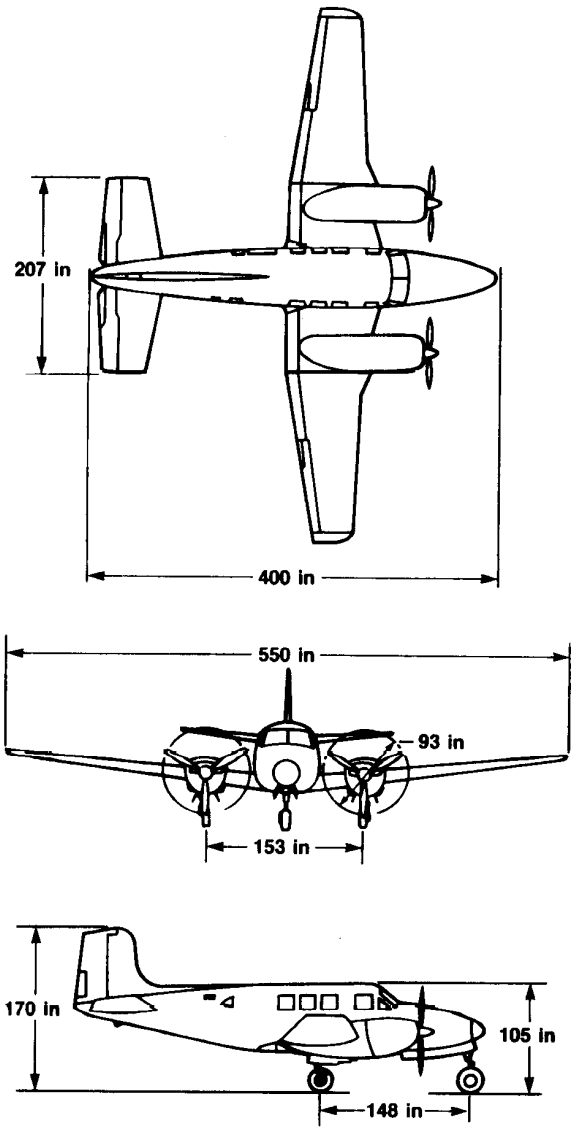

Figure 1. Three-view drawing of unmodified U-8F airplane.

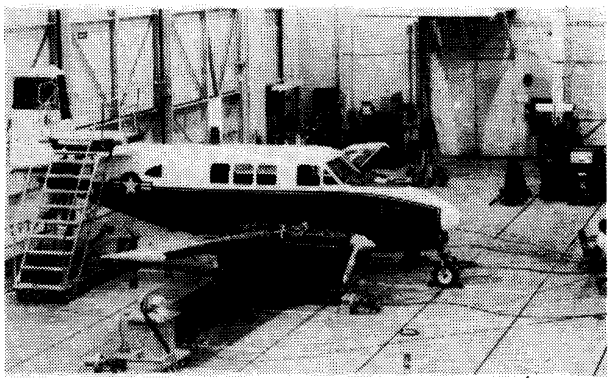

ECN 32776

Figure 2. Ground vibration test setup.

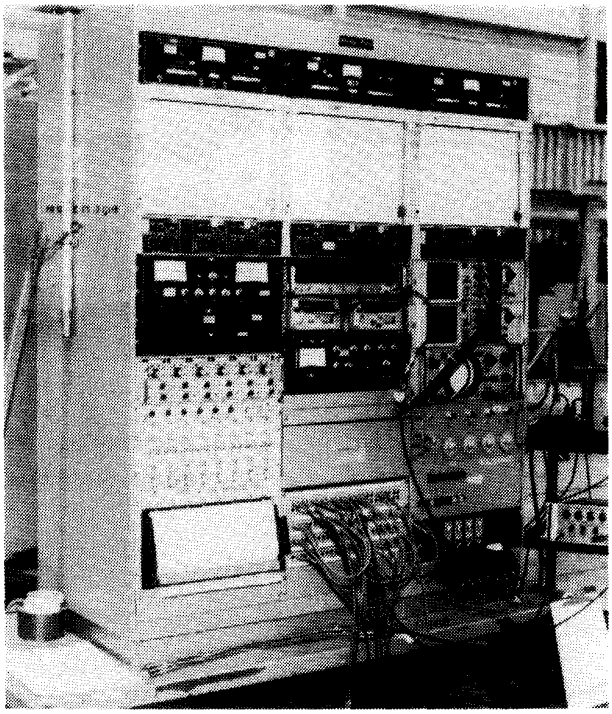

ECN 32760

Figure 3. Sine dwell ground vibration test equipment.

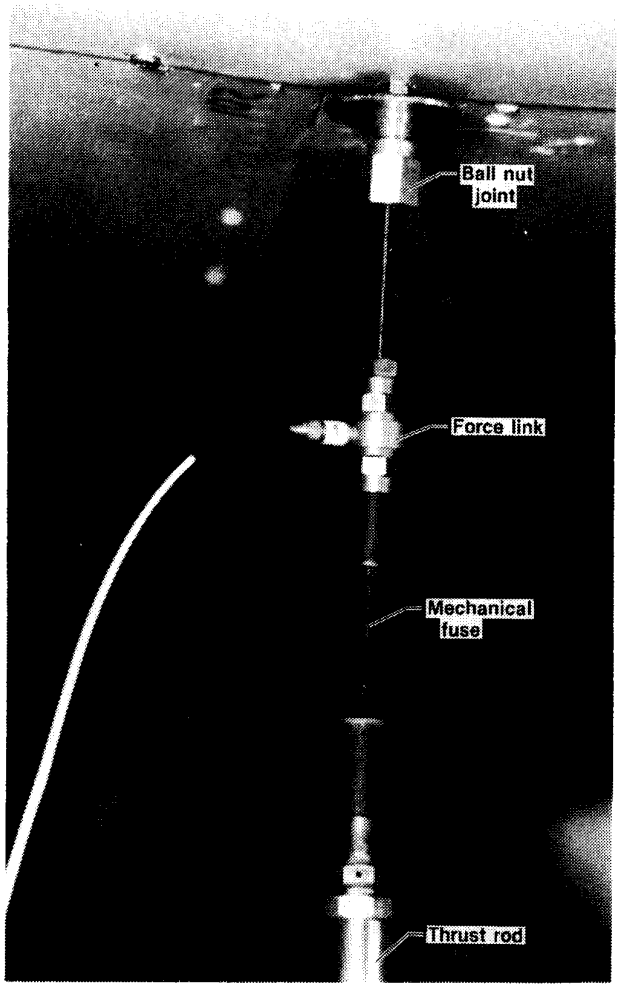

ECN 32759

Figure 4. Shaker attachment assembly.

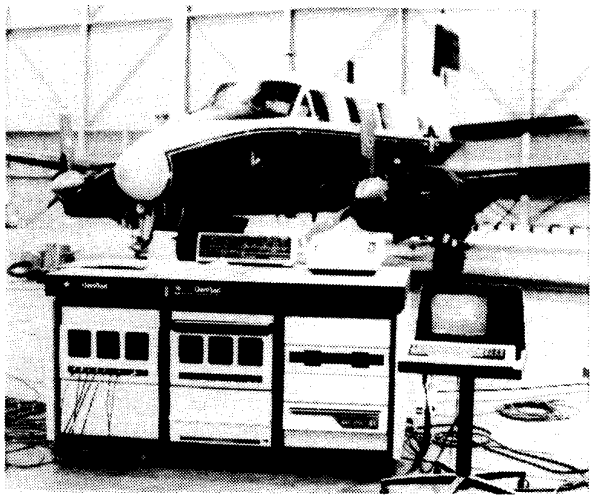

ECN 32762

Figure 5. Minicomputer-based structural analysis system.

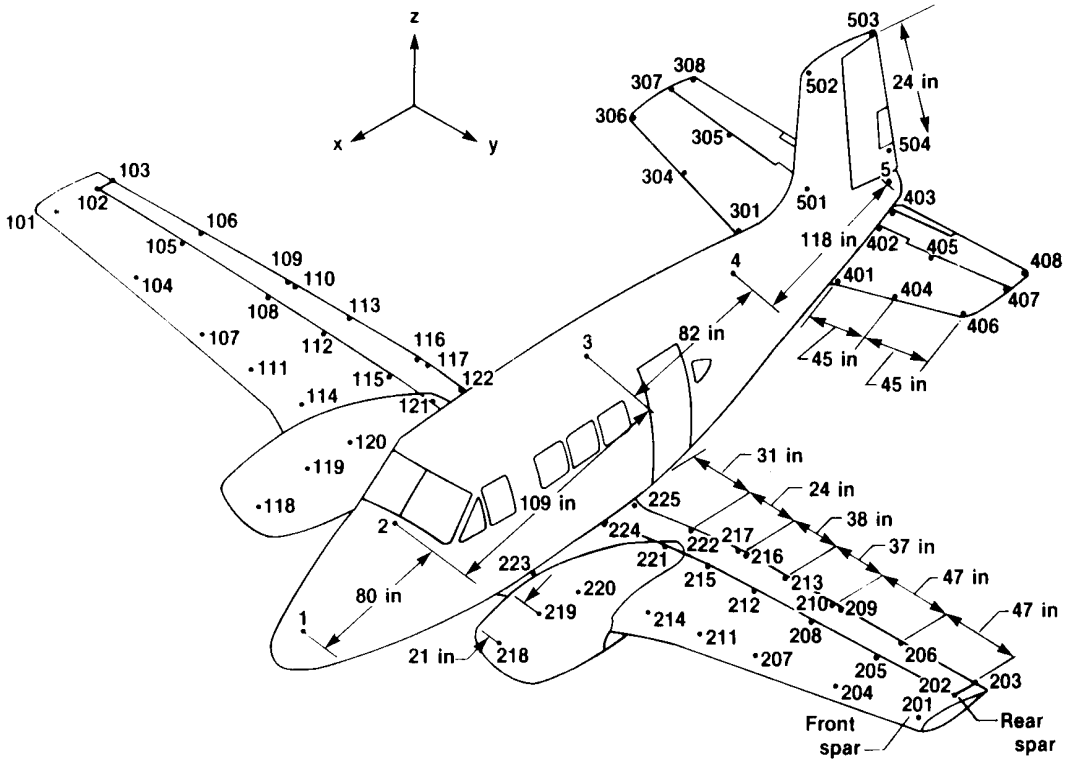

Figure 6. U-8F accelerometer locations for mode shape measurements.

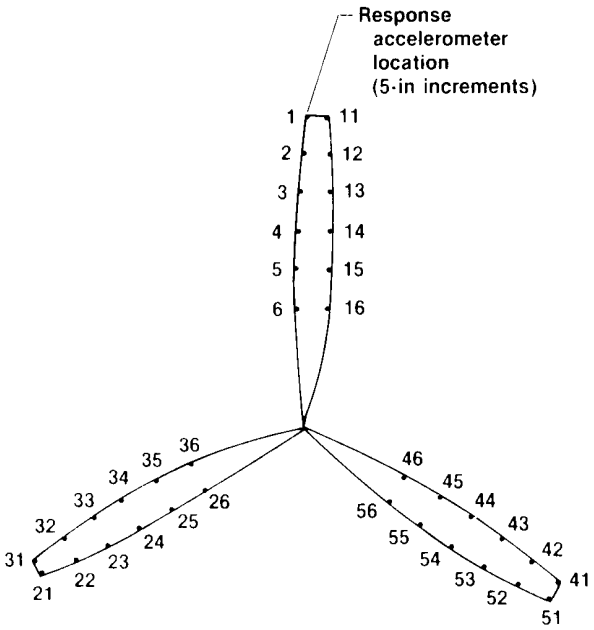

Figure 7. U-8F propeller impact hammer excitation locations.

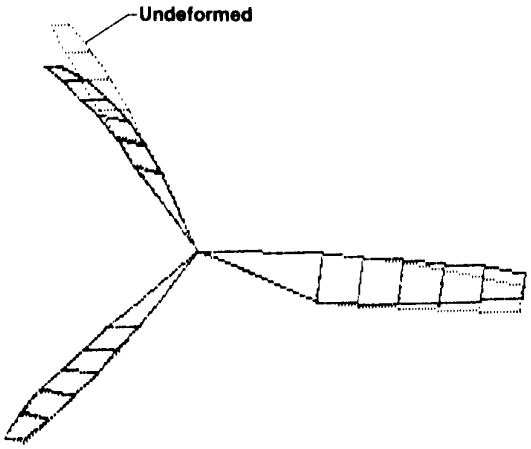

(a) 35.56-Hz frequency.

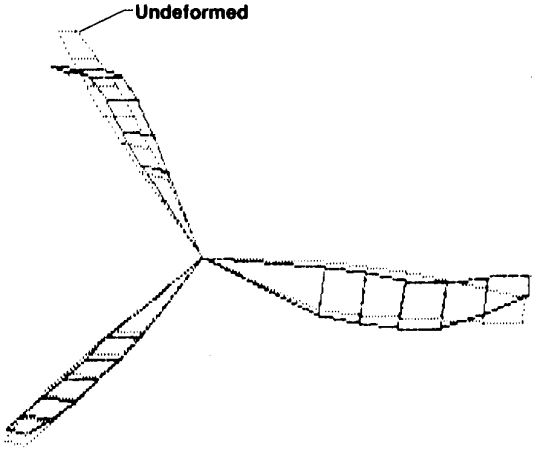

(b) 104.56-Hz frequency.

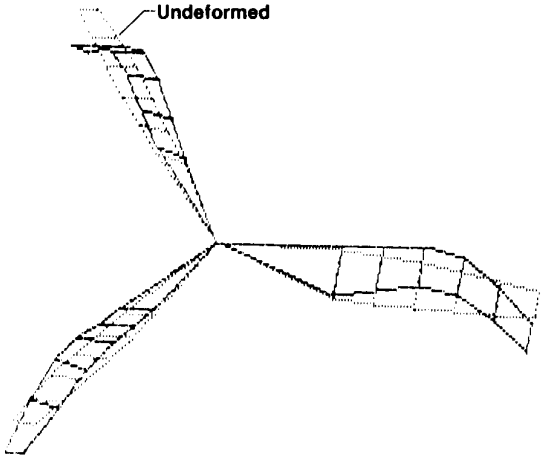

(c) 121.70-Hz frequency.

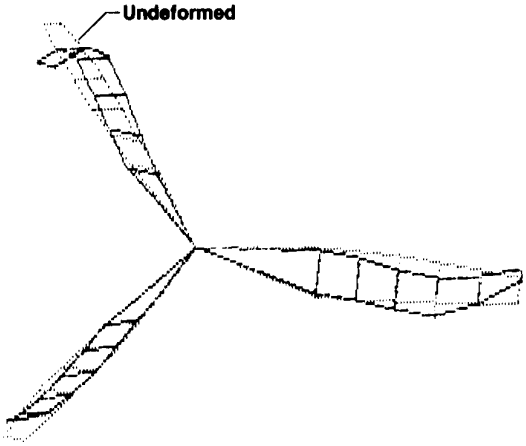

(d) 162.87-Hz frequency.

Figure 8. Propeller bending mode shapes.

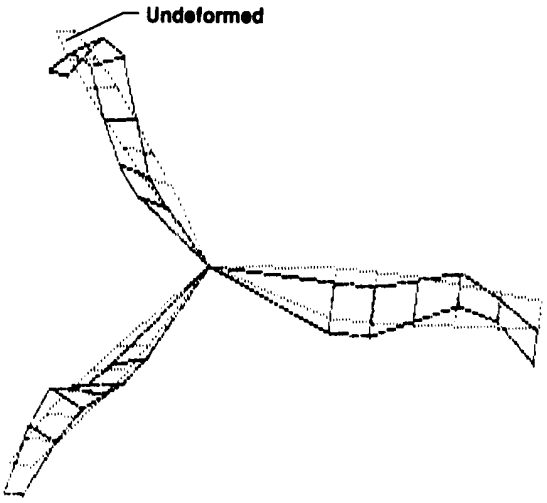

(e) 206.32-Hz frequency.

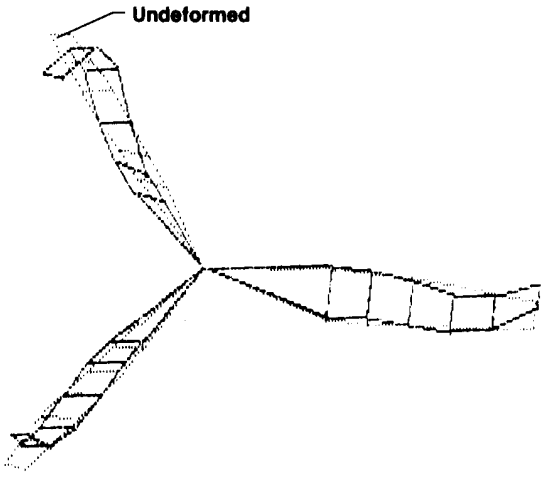

(f) 226.72-Hz frequency.

Figure 8. Concluded.

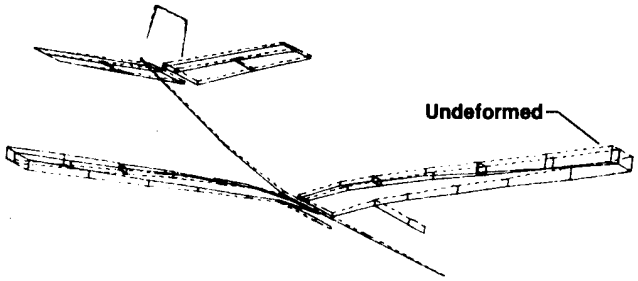

Figure 9. Rigid body roll mode shape (full fuel tanks), 3.17-Hz frequency.

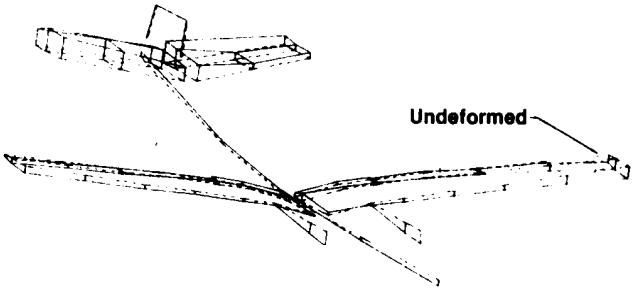

Figure 10. Rigid body pitch mode shape (full fuel tanks), 4.17-Hz frequency.

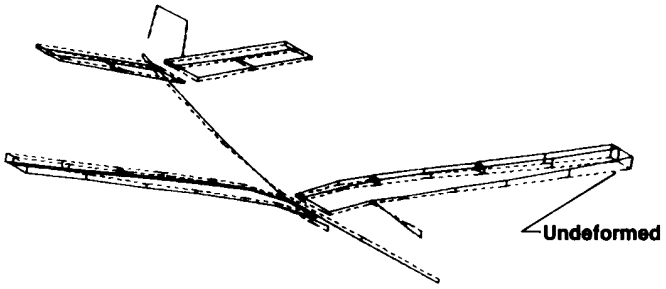

Figure 11. Antisymmetric engine pitch mode shape (full fuel tanks), 6.76-Hz frequency.

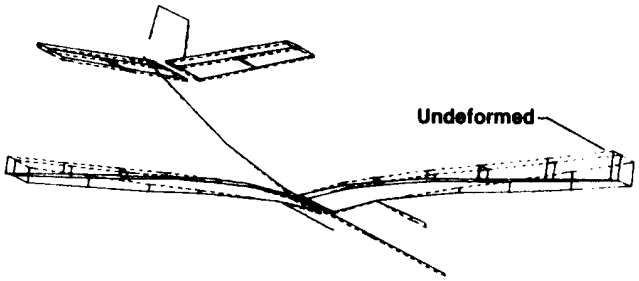

Figure 12. Symmetric wing bending mode shape (full fuel tanks), 6.86-Hz frequency.

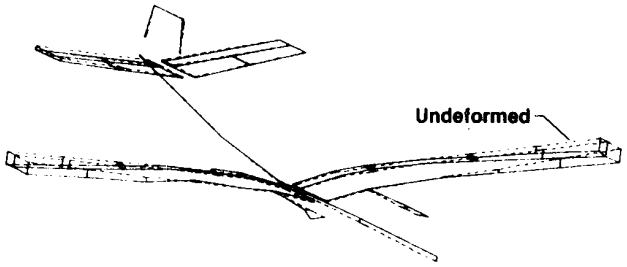

Figure 13. Symmetric engine lateral mode shape (full fuel tanks), 8.03-Hz frequency.

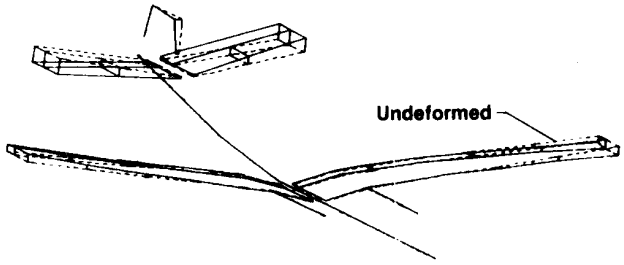

Figure 14. Fuselage torsion mode shape (full fuel tanks), 10.19-Hz frequency.

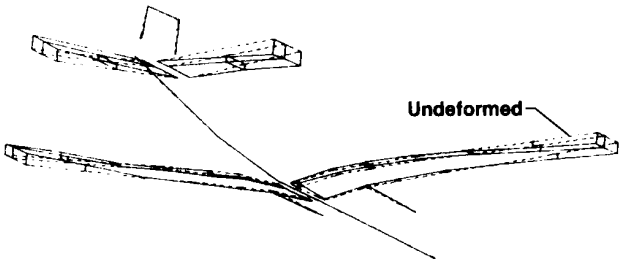

Figure 15. Antisymmetric wing bending mode shape (full fuel tanks), 14.98-Hz frequency.

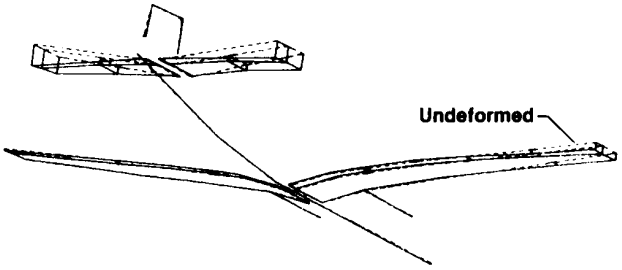

Figure 16. Symmetric horizontal stabilizer bending mode shape (full fuel tanks), 15.99-Hz frequency.

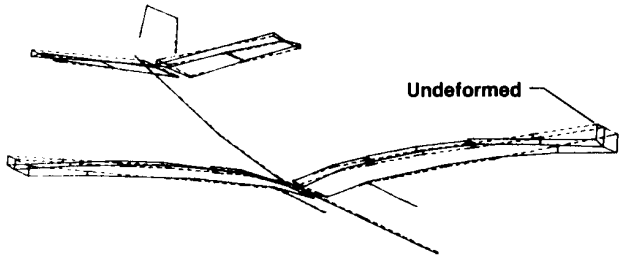

Figure 17. Symmetric second wing bending mode shape (full fuel tanks), 19.14-Hz frequency.

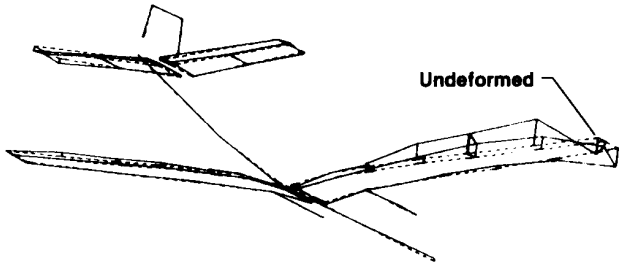

Figure 18. Wing torsion mode shape (full fuel tanks), 34.30-Hz frequency.

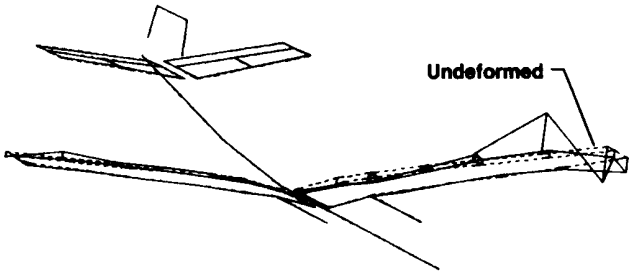

Figure 19. Aileron bending mode shape (full fuel tanks), 41.18-Hz frequency.

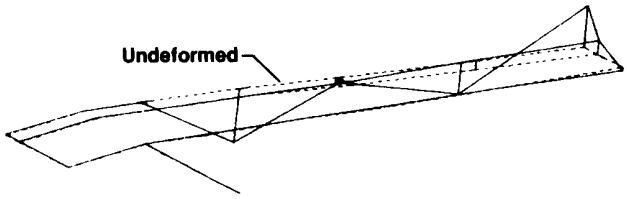

(a) 65.62-Hz frequency.

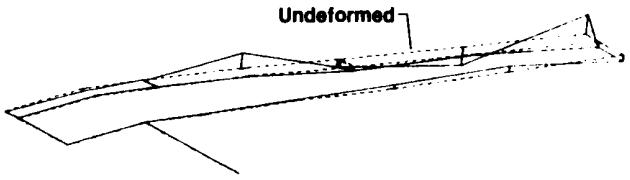

(b) 89.57-Hz frequency.

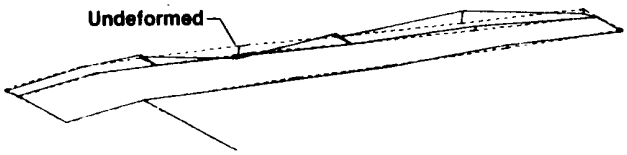

(c) 107.09-Hz frequency.

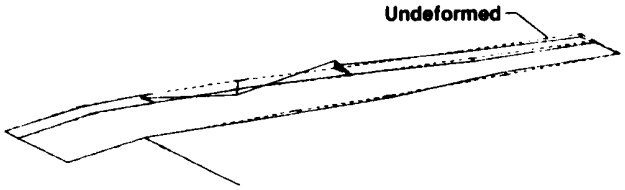

(d) 110.06-Hz frequency.

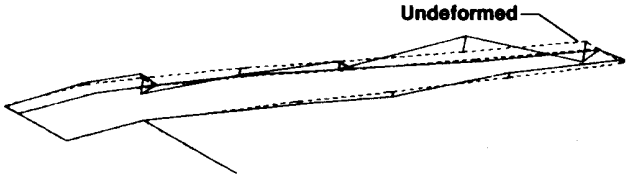

(e) 120.56-Hz frequency.

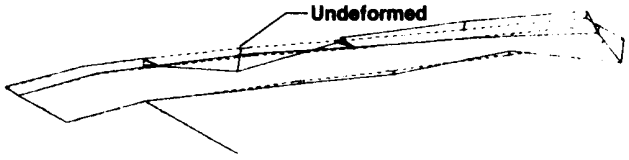

(f) 132.12-Hz frequency.

Figure 20. Left wing control surface mode shapes (full fuel tanks).

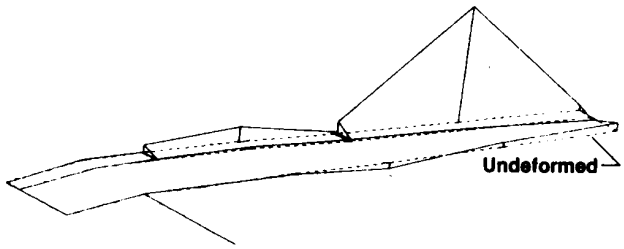

(g) 143.32-Hz frequency.

Figure 20. Concluded.

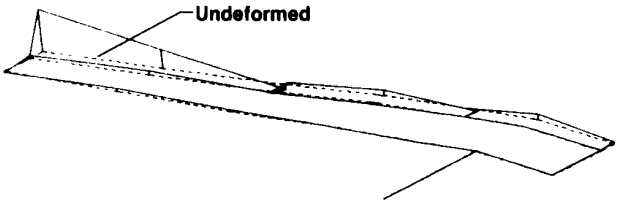

(a) 67.99-Hz frequency.

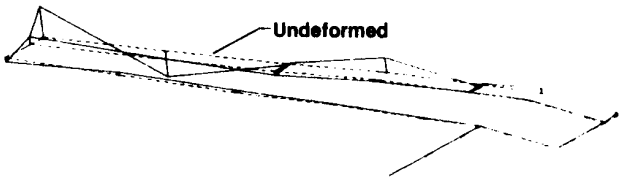

(b) 84.54-Hz frequency.

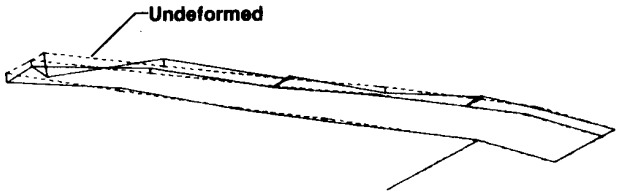

(c) 111.93-Hz frequency.

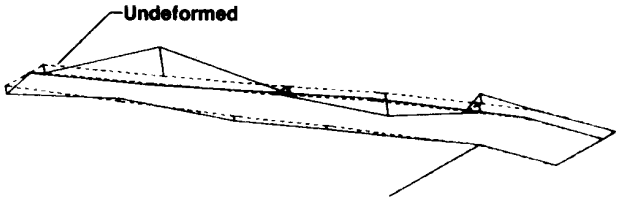

(d) 121.80-Hz frequency.

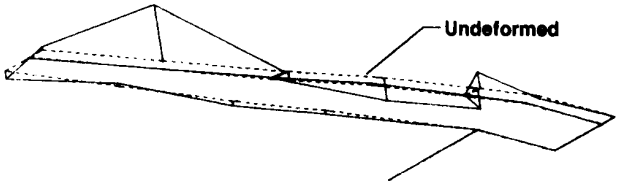

(e) 123.21-Hz frequency.

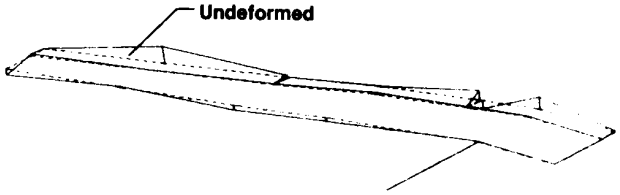

(f) 125.17-Hz frequency.

Figure 21. Right wing control surface mode shapes (full fuel tanks).

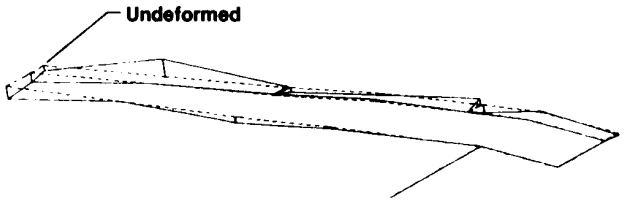

(g) 137.86-Hz frequency.

Figure 21. Concluded.

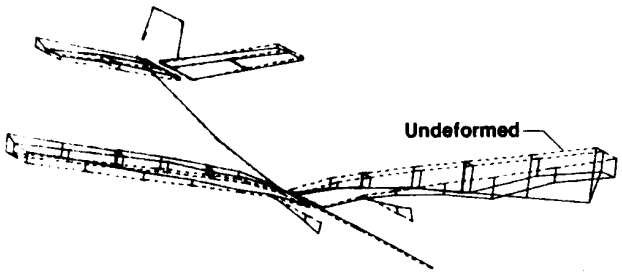

Figure 22. Antisymmetric engine pitch mode shape (empty fuel tanks), 7.02-Hz frequency.

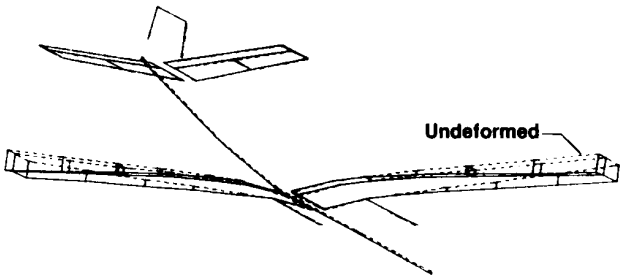

Figure 23. Symmetric wing bending mode shape (empty fuel tanks), 8.03-Hz frequency.

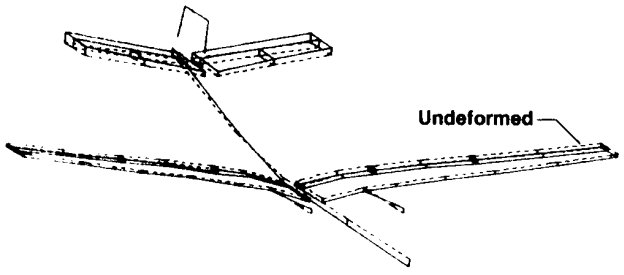

Figure 24. Symmetric engine pitch mode shape (empty fuel tanks), 9.47-Hz frequency.

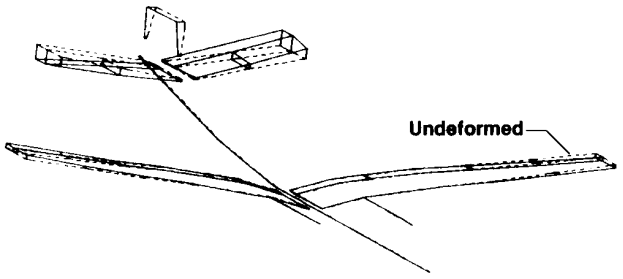

Figure 25. Fuselage torsion mode shape (empty fuel tanks), 10.56-Hz frequency.

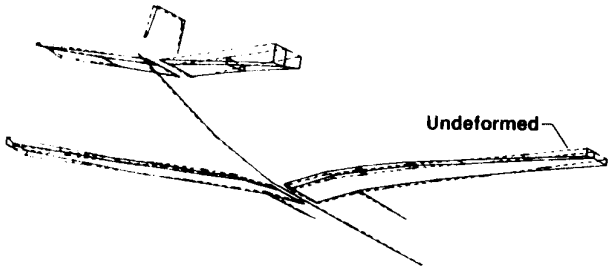

Figure 26. Symmetric horizontal stabilizer bending mode shape (empty fuel tanks), 15.88-Hz frequency.

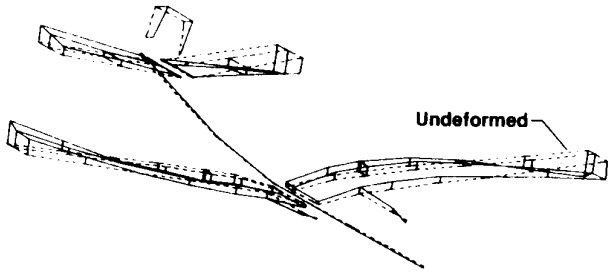

Figure 27. Antisymmetric wing bending mode shape (empty fuel tanks), 16.25-Hz frequency.

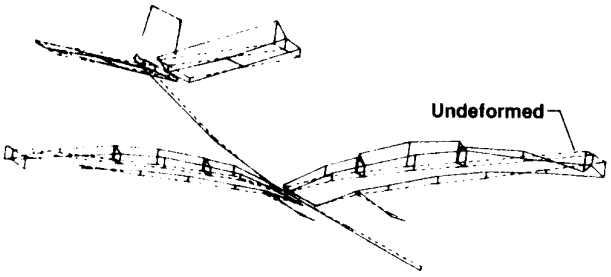

Figure 28. Symmetric second wing bending mode shape (empty fuel tanks), 24.64-Hz frequency.

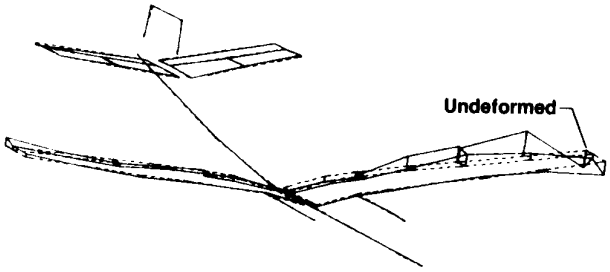

Figure 29. Wing torsion mode shape (empty fuel tanks), 38.02-Hz frequency.

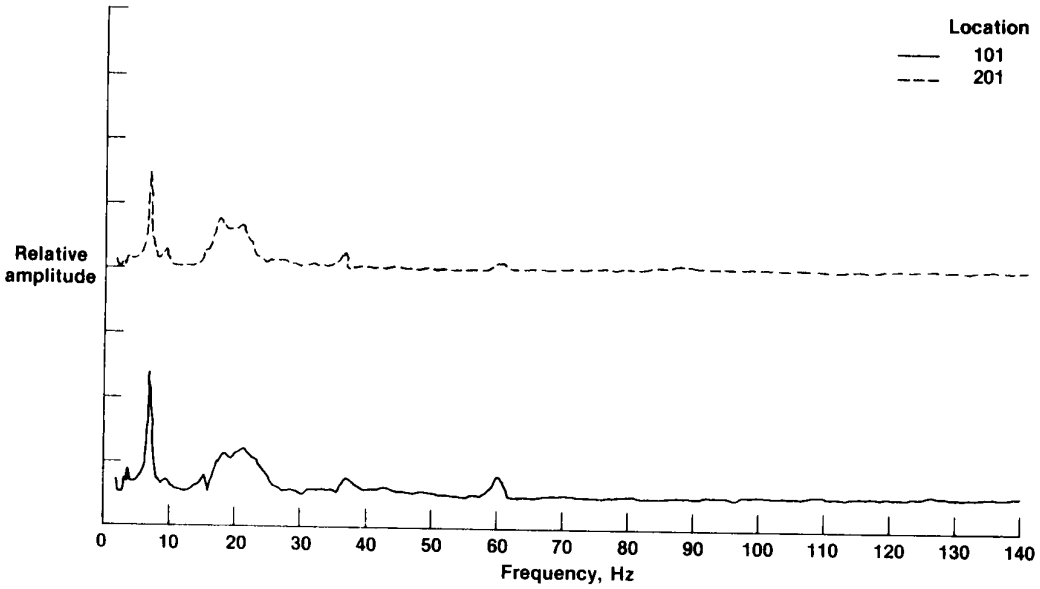

Figure 30. Location 101 and 201 vertical frequency responses due to symmetric sweep at each engine (full fuel tanks).

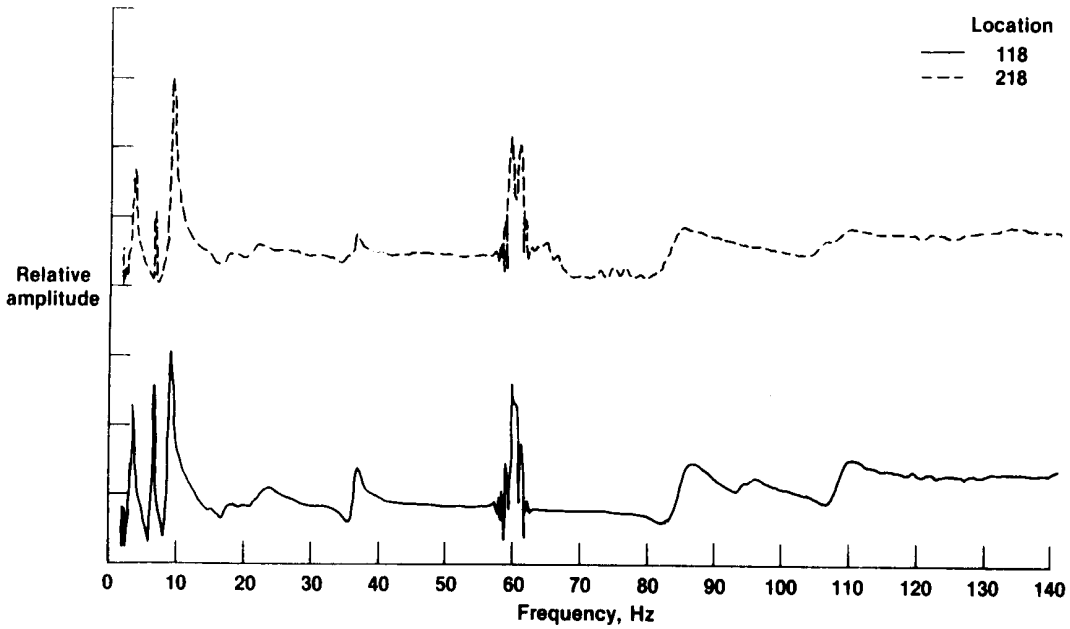

Figure 31. Location 118 and 218 vertical frequency responses due to symmetric sweep at each engine (full fuel tanks).

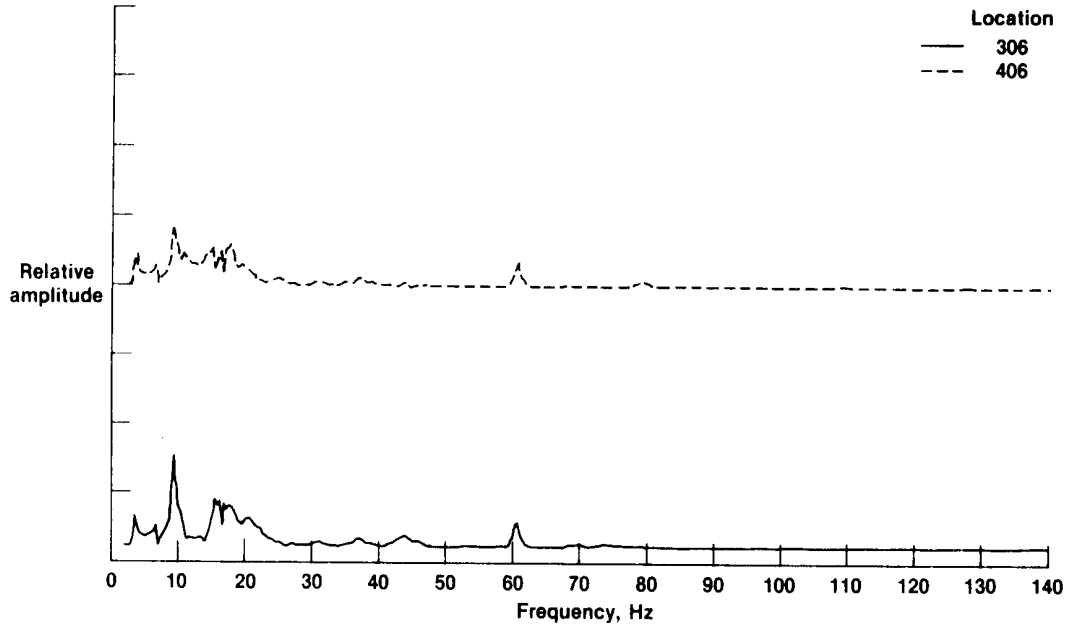

Figure 32. Location 306 and 406 vertical frequency responses due to symmetric sweep at each engine (full fuel tanks).

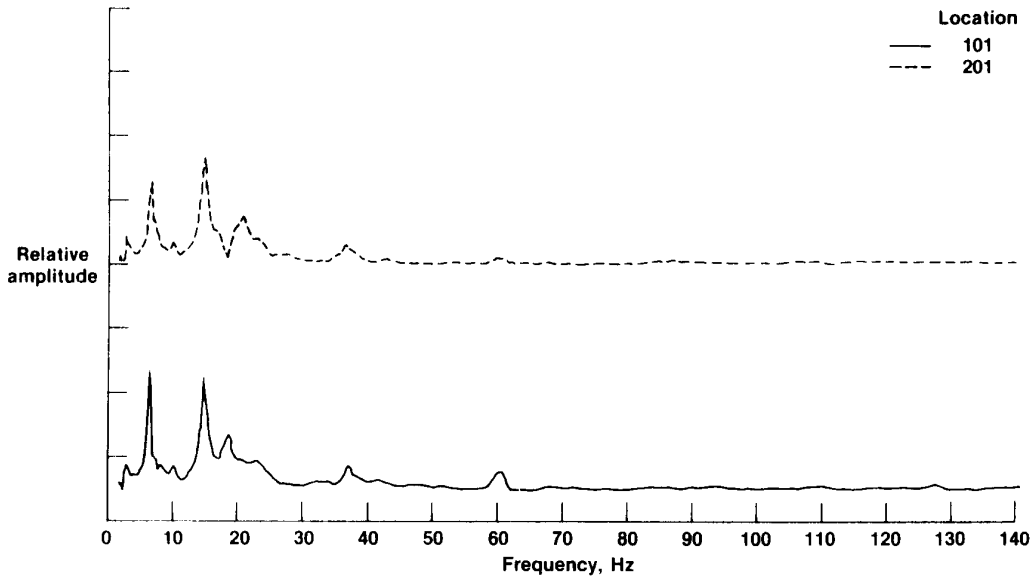

Figure 33. Location 101 and 201 vertical frequency responses due to antisymmetric sweep at each engine (full fuel tanks).

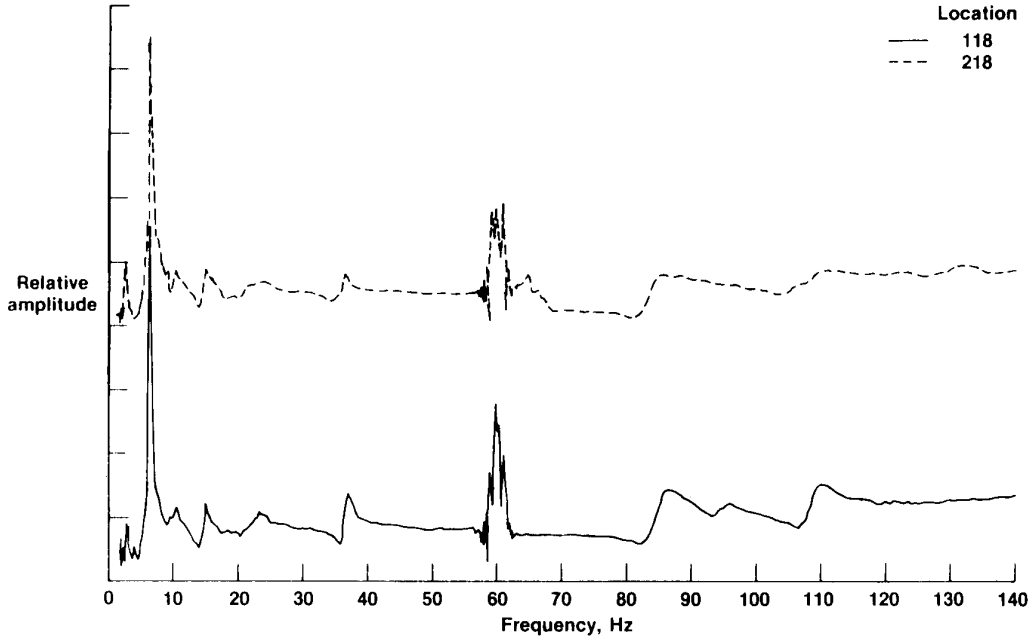

Figure 34. Location 118 and 218 vertical frequency responses due to antisymmetric sweep at each engine (full fuel tanks).

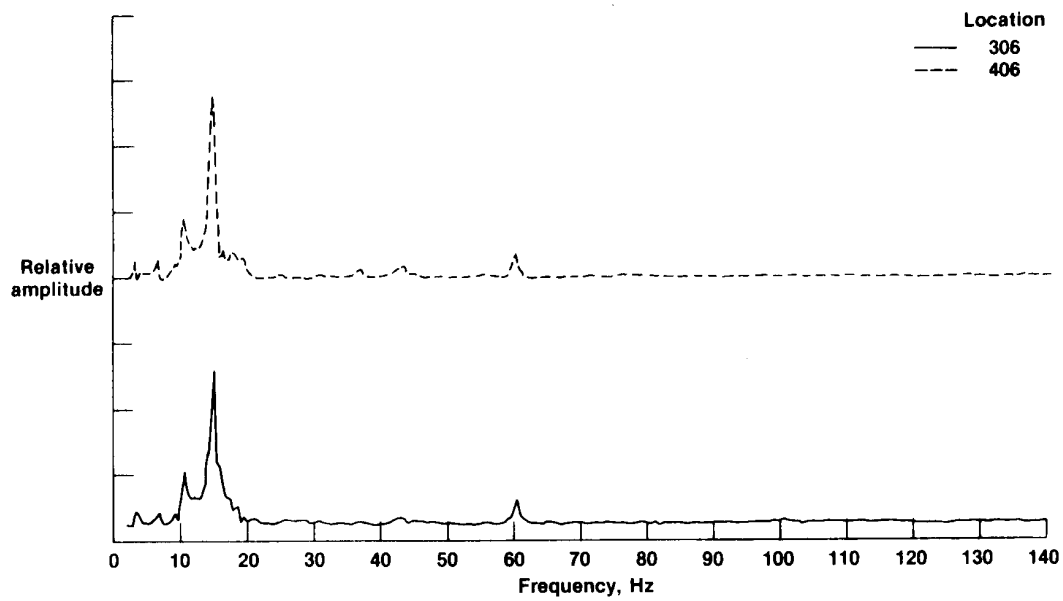

Figure 35. Location 306 and 406 vertical frequency responses due to antisymmetric sweep at each engine (full fuel tanks).

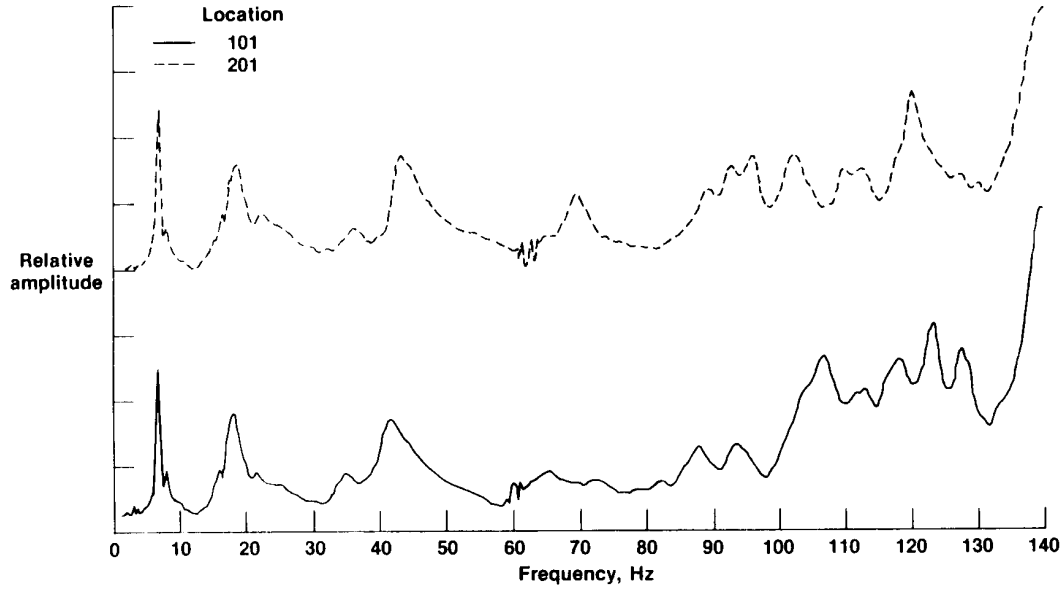

Figure 36. Location 101 and 201 vertical frequency responses due to symmetric sweep at each wingtip (full fuel tanks).

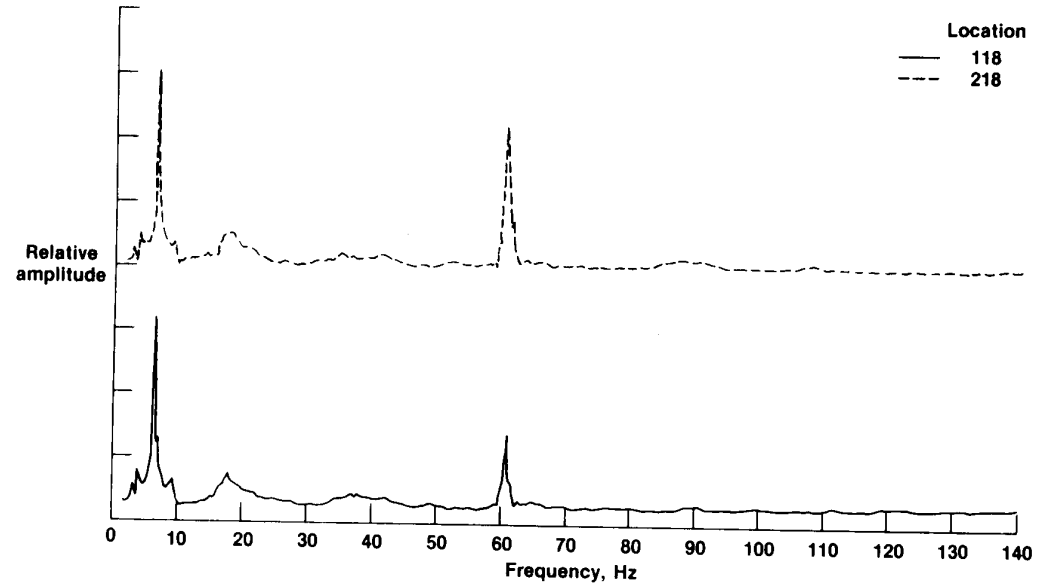

Figure 37. Location 118 and 218 vertical frequency responses due to symmetric sweep at each wingtip (full fuel tanks).

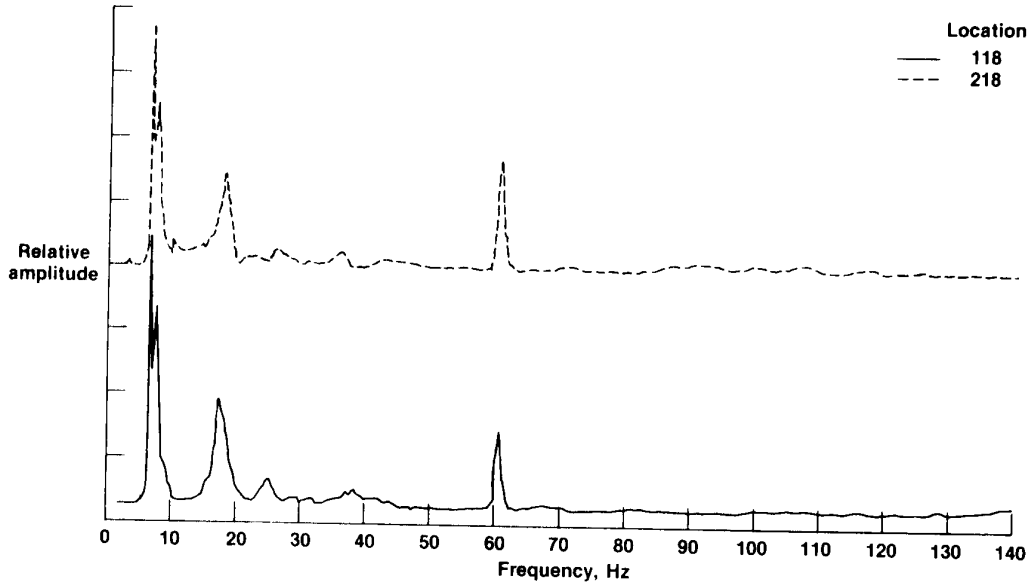

Figure 38. Location 118 and 218 lateral frequency responses due to symmetric sweep at each wingtip (full fuel tanks).

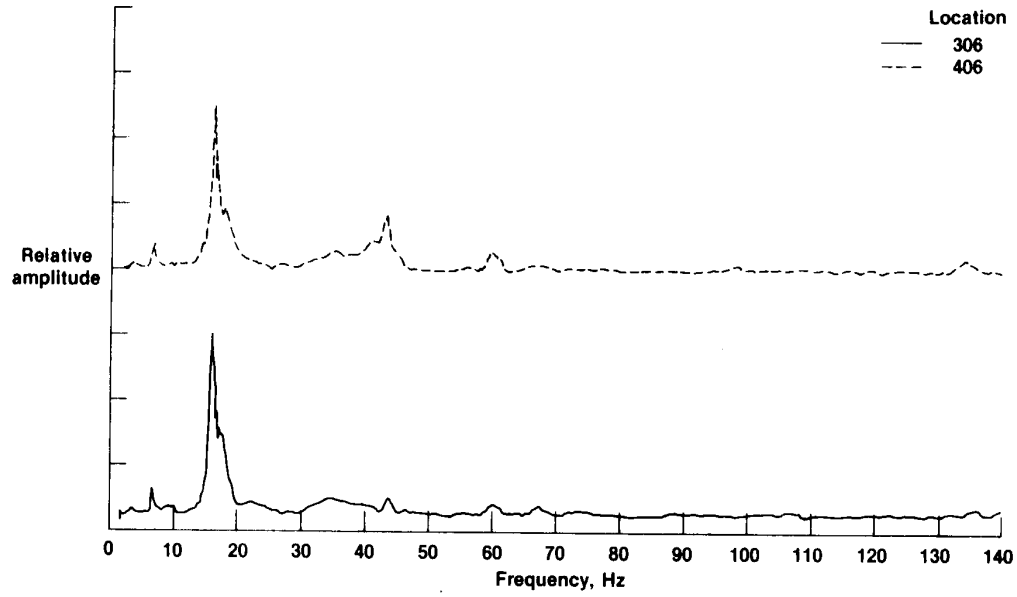

Figure 39. Location 306 and 406 vertical frequency responses due to symmetric sweep at each wingtip (full fuel tanks).

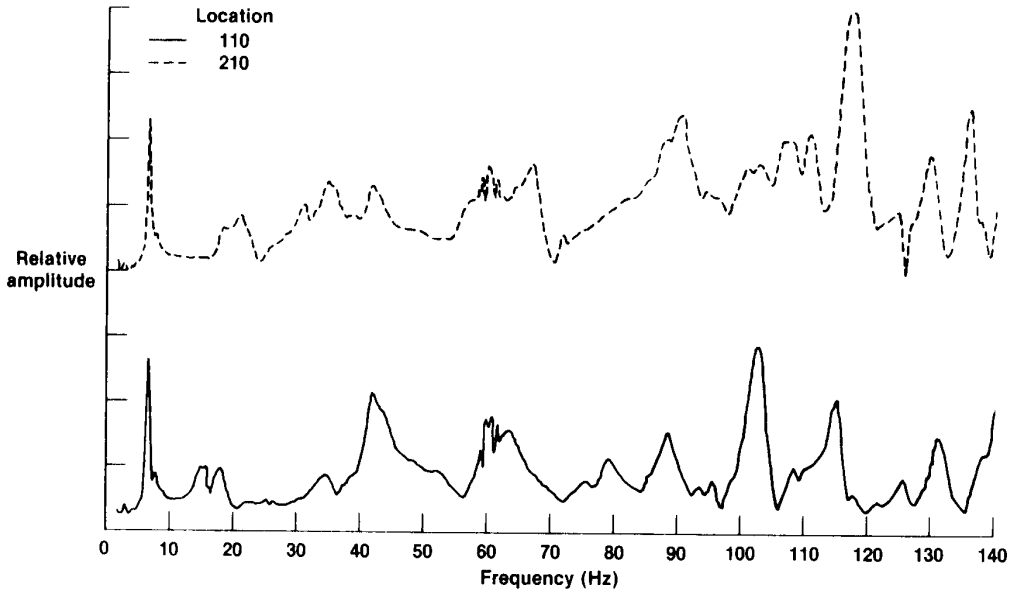

Figure 40. Location 110 and 210 vertical frequency responses due to symmetric sweep at each wingtip (full fuel tanks).

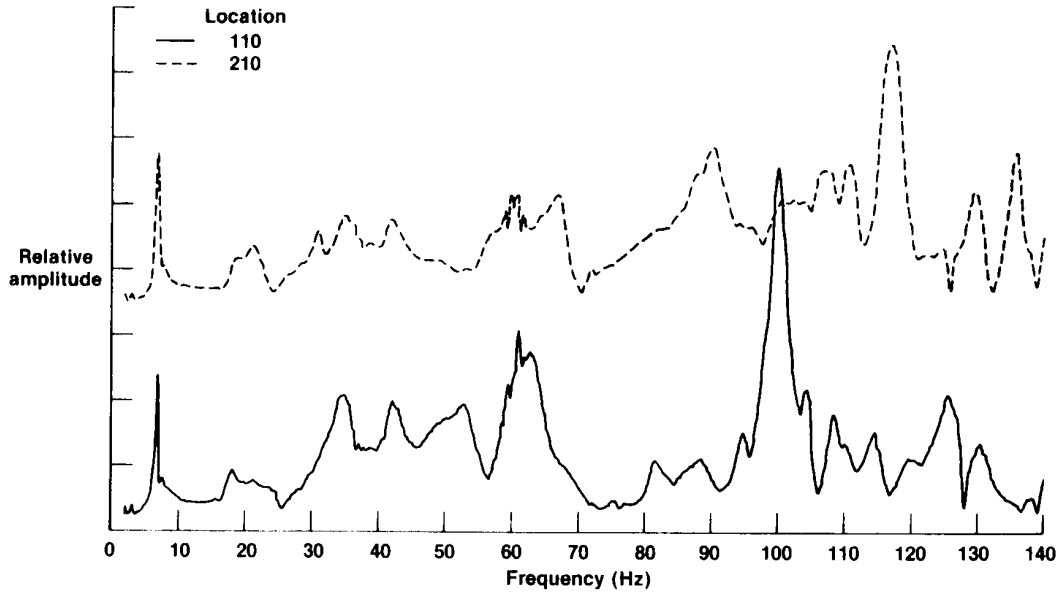

Figure 41. Location 110 and 210 vertical frequency responses (10-lb preload) due to symmetric sweep at each wingtip (full fuel tanks).

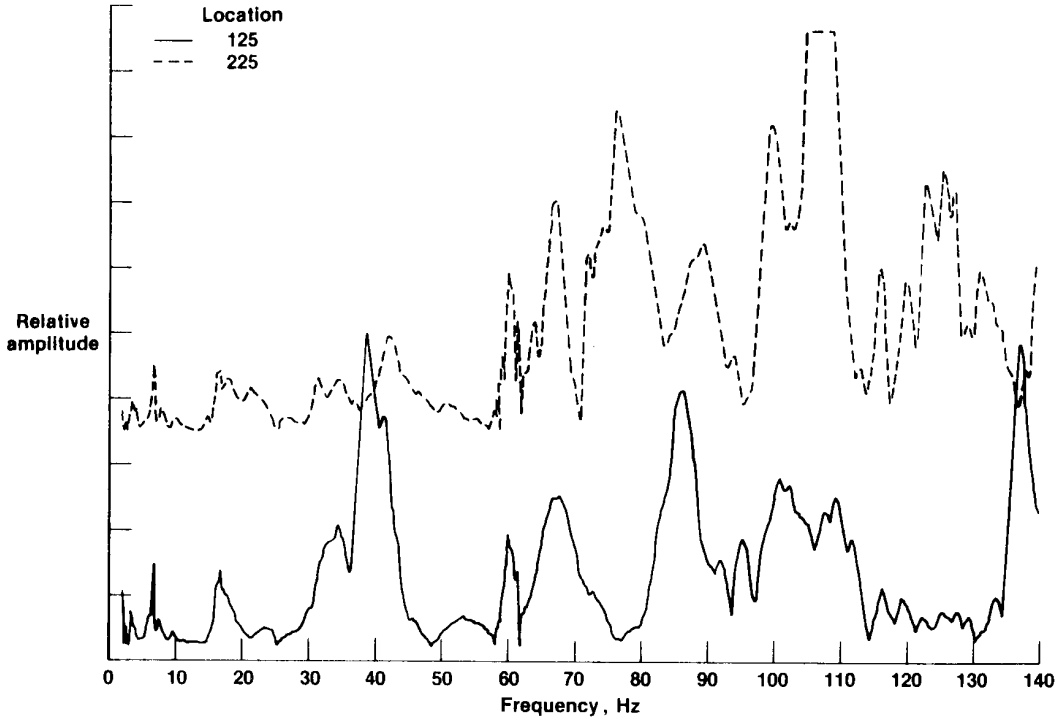

Figure 42. Location 125 and 225 vertical frequency responses due to symmetric sweep at each wingtip (full fuel tanks).

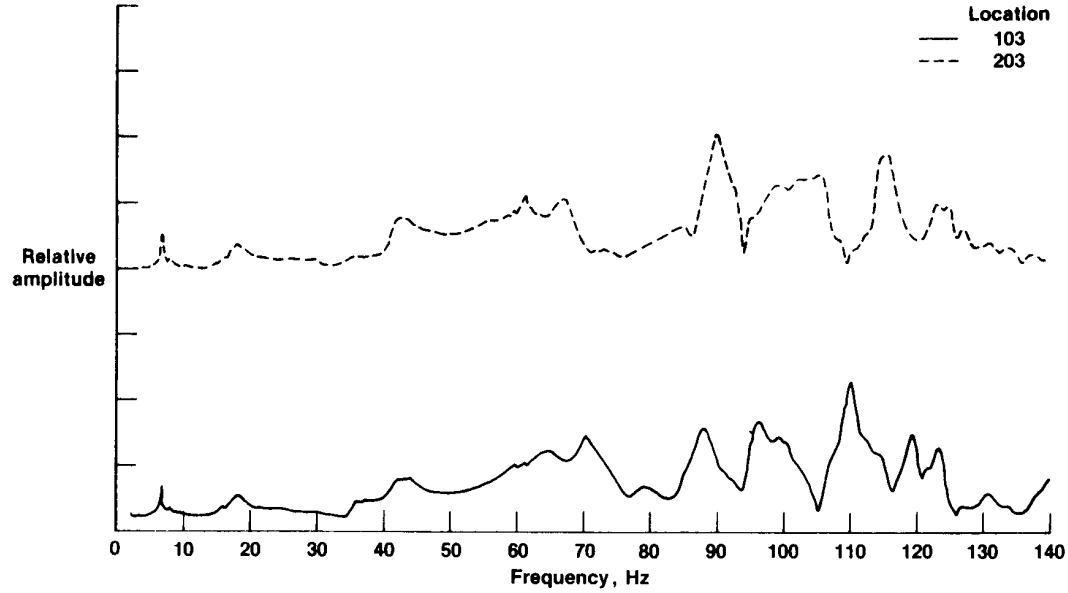

Figure 43. Location 103 and 203 vertical frequency responses due to symmetric sweep at each wingtip (full fuel tanks).

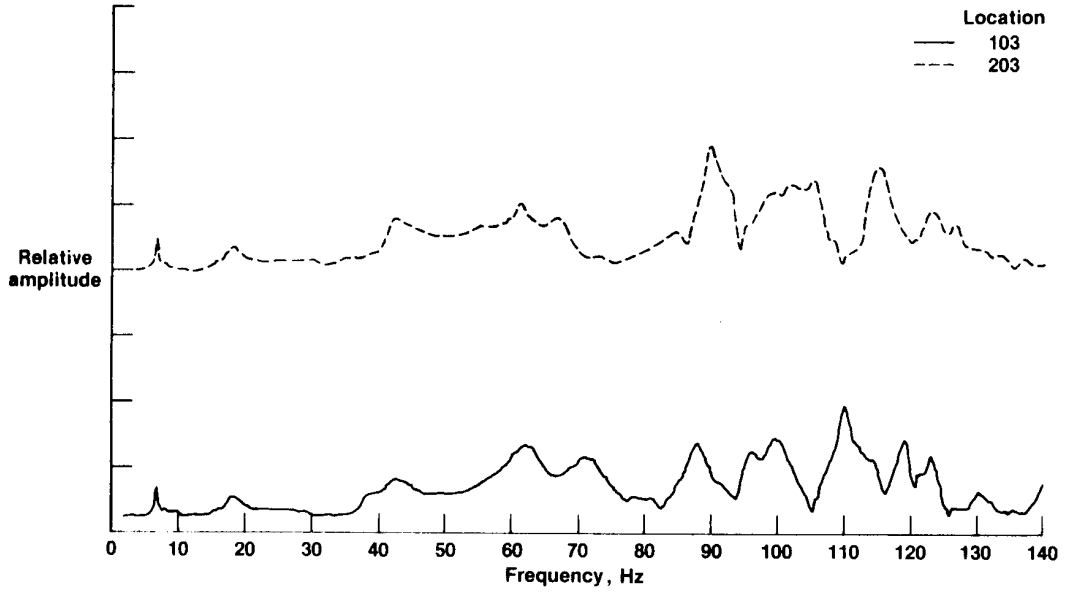

Figure 44. Location 103 and 203 vertical frequency responses (10-lb preload) due to symmetric sweep at each wingtip (full fuel tanks).

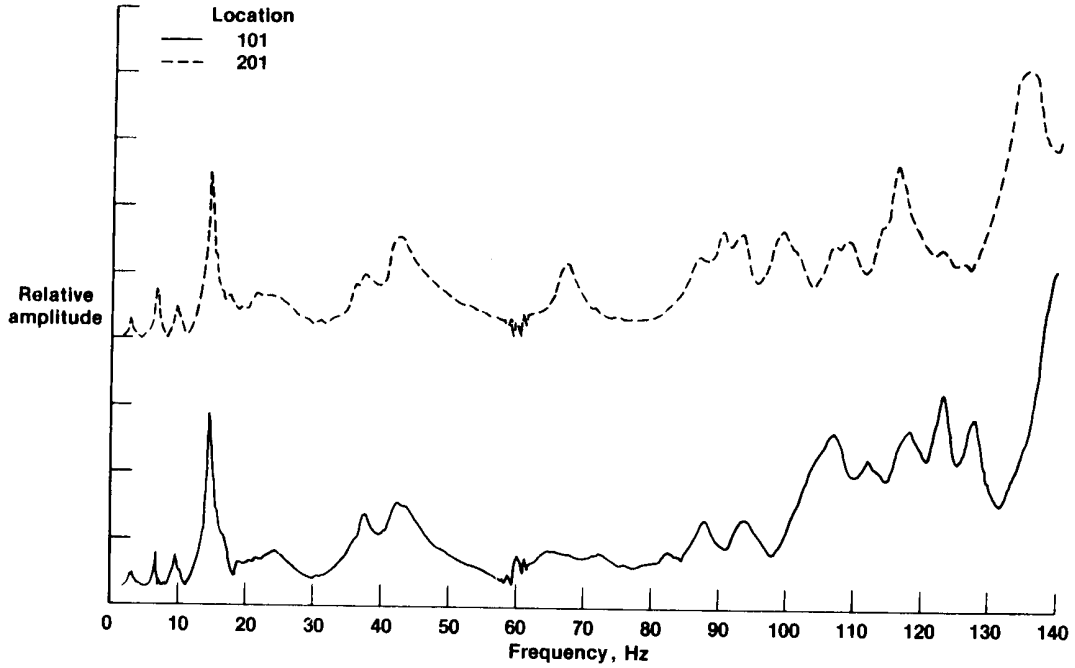

Figure 45. Location 101 and 201 vertical frequency responses due to antisymmetric sweep at each wingtip (full fuel tanks).

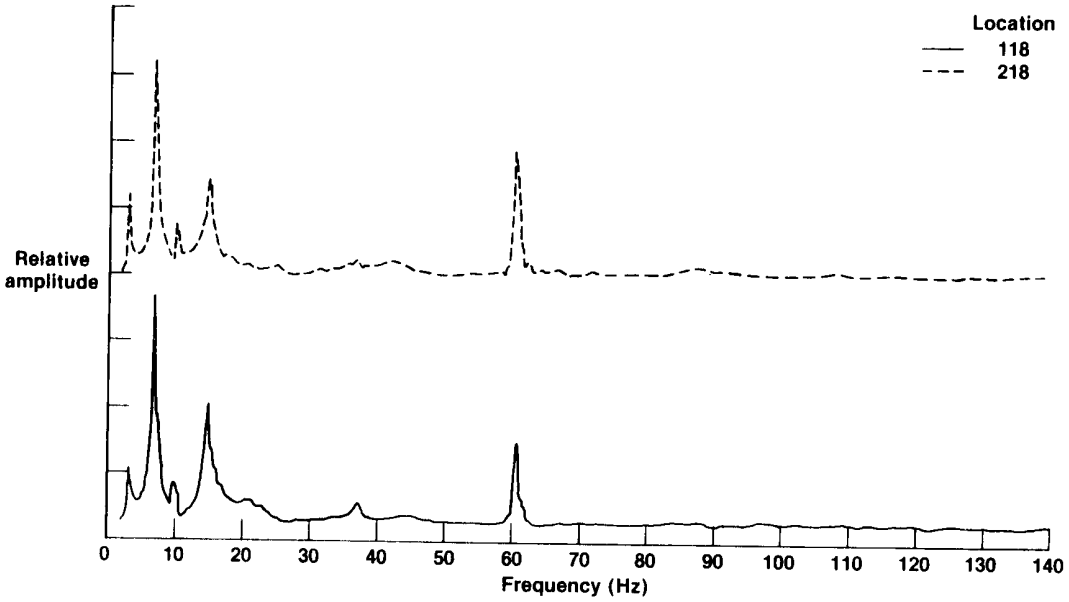

Figure 46. Location 118 and 218 vertical frequency responses due to antisymmetric sweep at each wingtip (full fuel tanks).

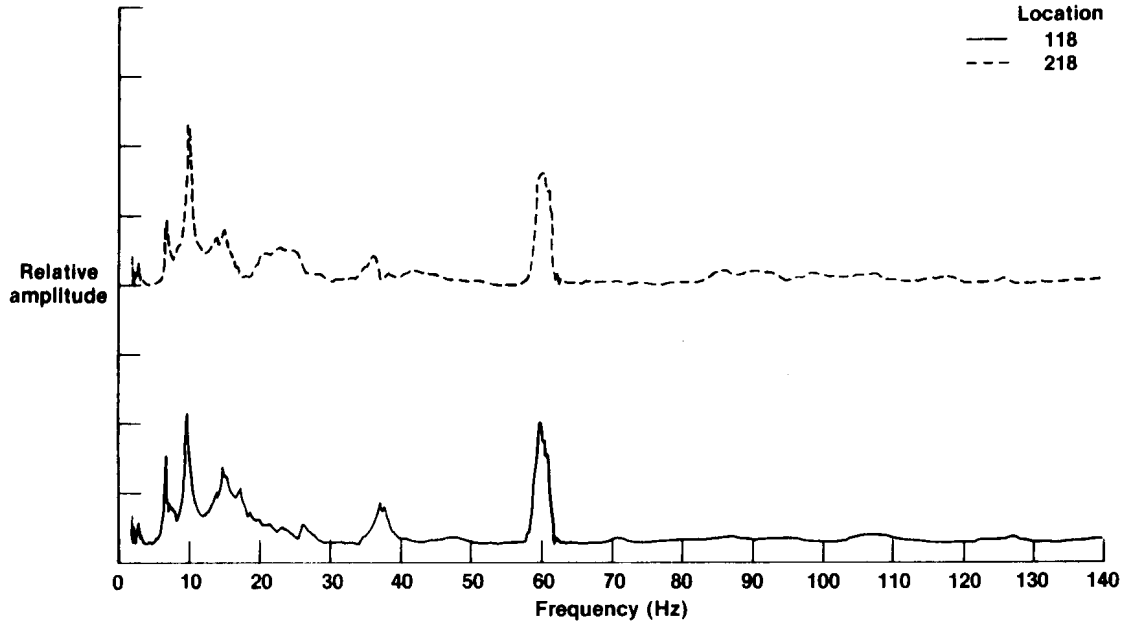

Figure 47. Location 118 and 218 lateral frequency responses due to antisymmetric sweep at each wingtip (full fuel tanks).

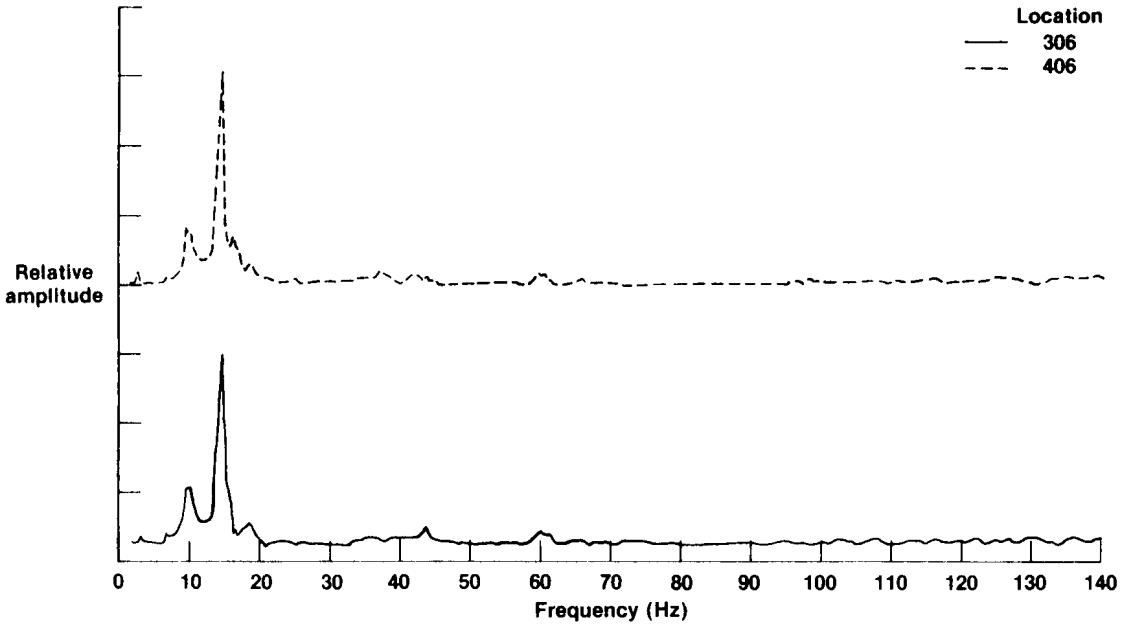

Figure 48. Location 306 and 406 vertical frequency responses due to antisymmetric sweep at each wingtip (full fuel tanks).

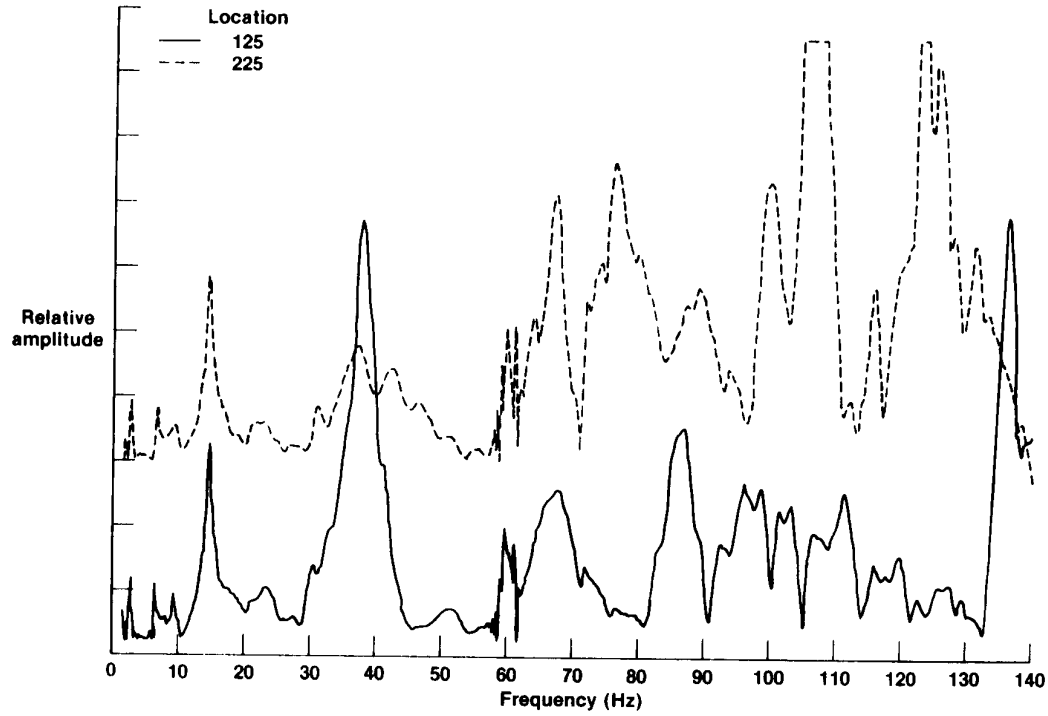

Figure 49. Location 125 and 225 vertical frequency responses due to antisymmetric sweep at each wingtip (full fuel tanks).

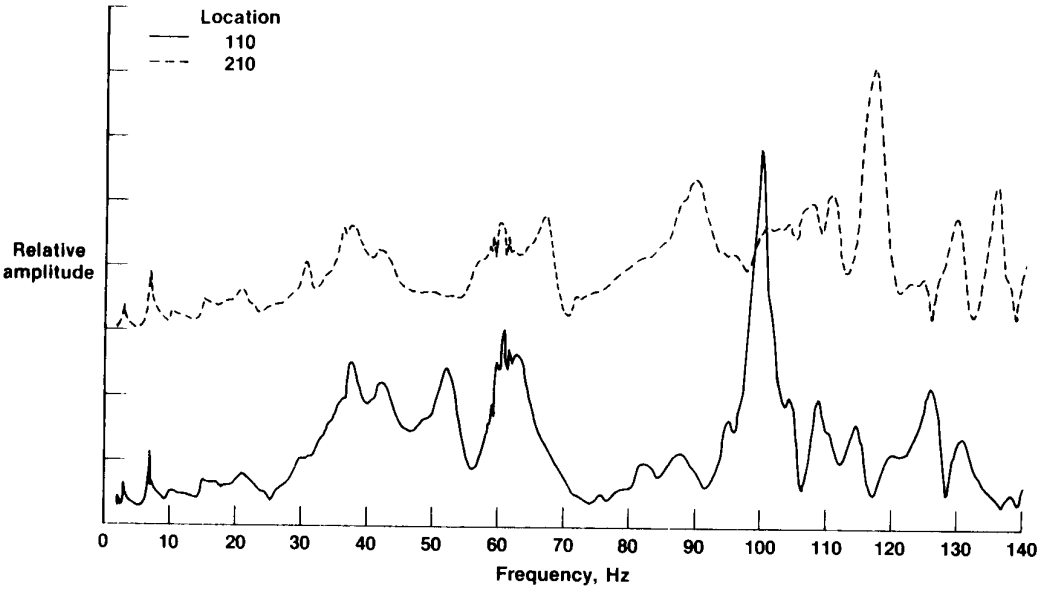

Figure 50. Location 110 and 210 vertical frequency responses (10-lb preload) due to antisymmetric sweep at each wingtip (full fuel tanks).

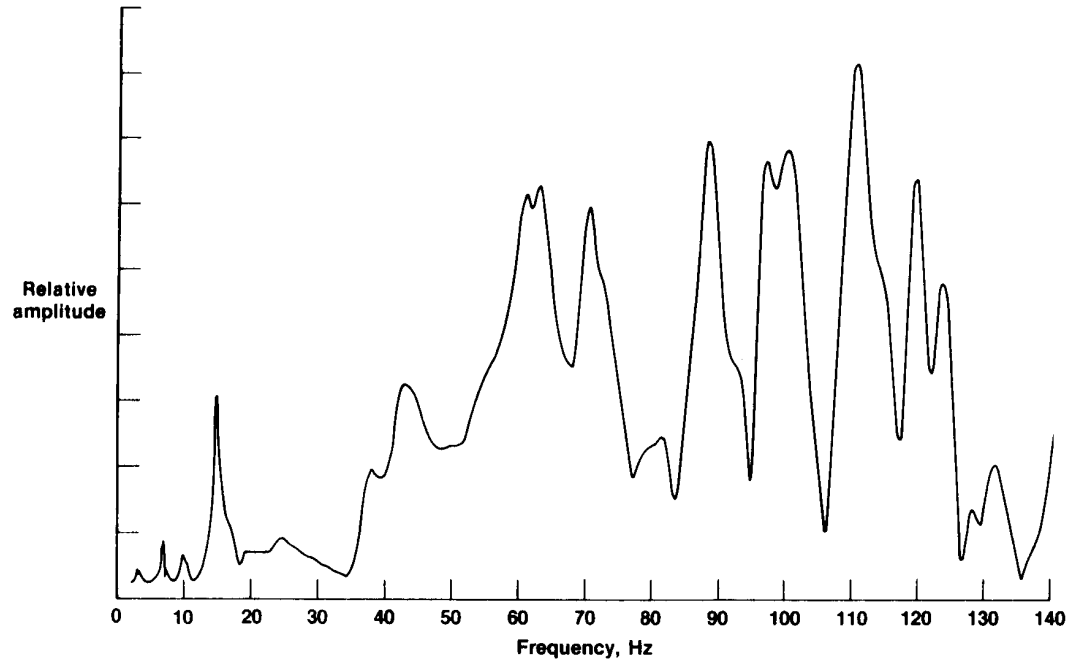

Figure 51. Location 103 vertical frequency response due to antisymmetric sweep at each wingtip (full fuel tanks).

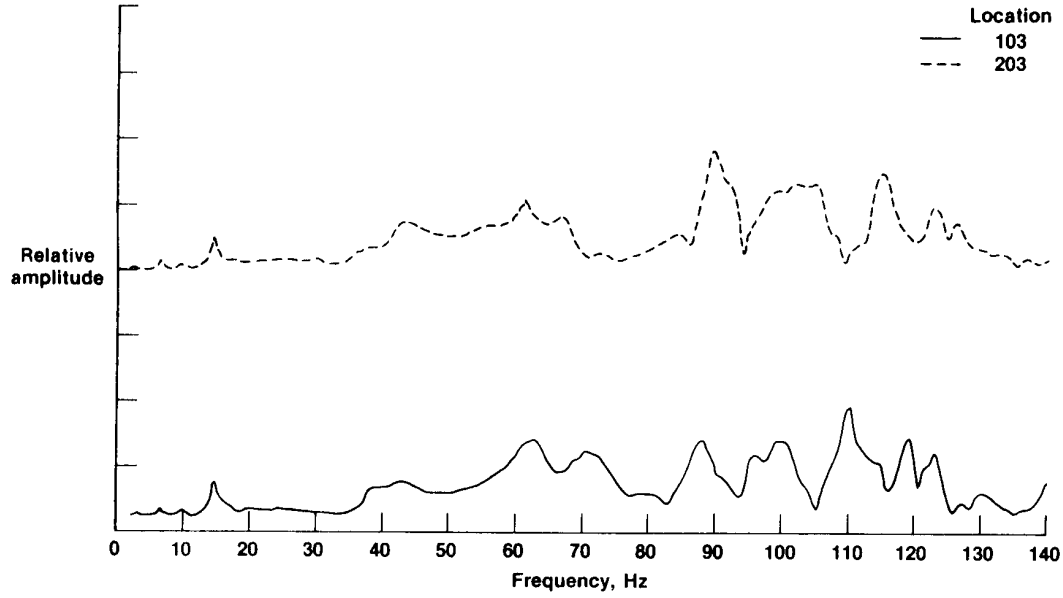

Figure 52. Location 103 and 203 frequency responses (10-lb preload) due to antisymmetric sweep at each wingtip (full fuel tanks).

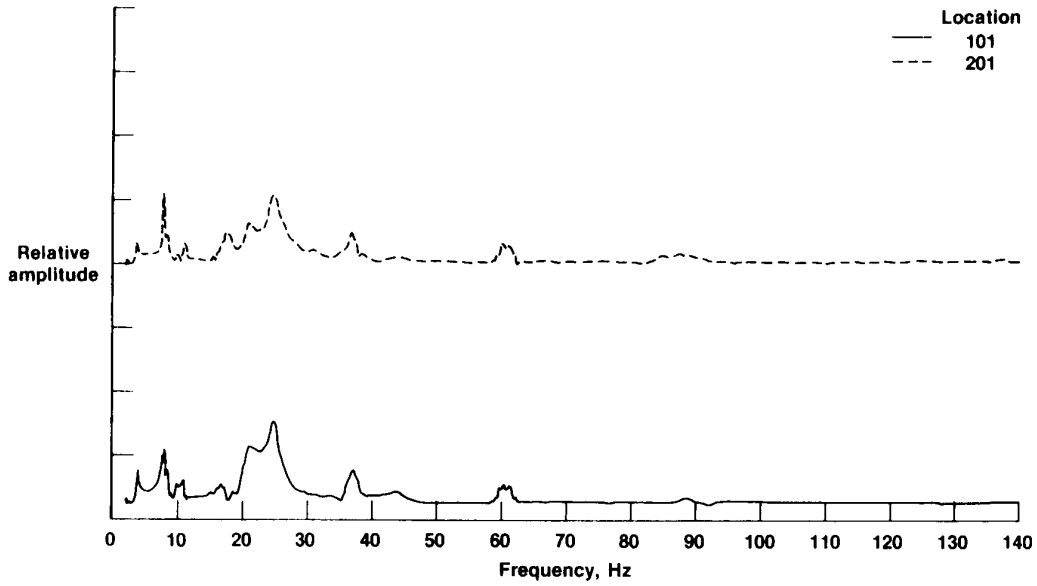

Figure 53. Location 101 and 201 vertical frequency responses due to symmetric sweep at each engine (empty fuel tanks).

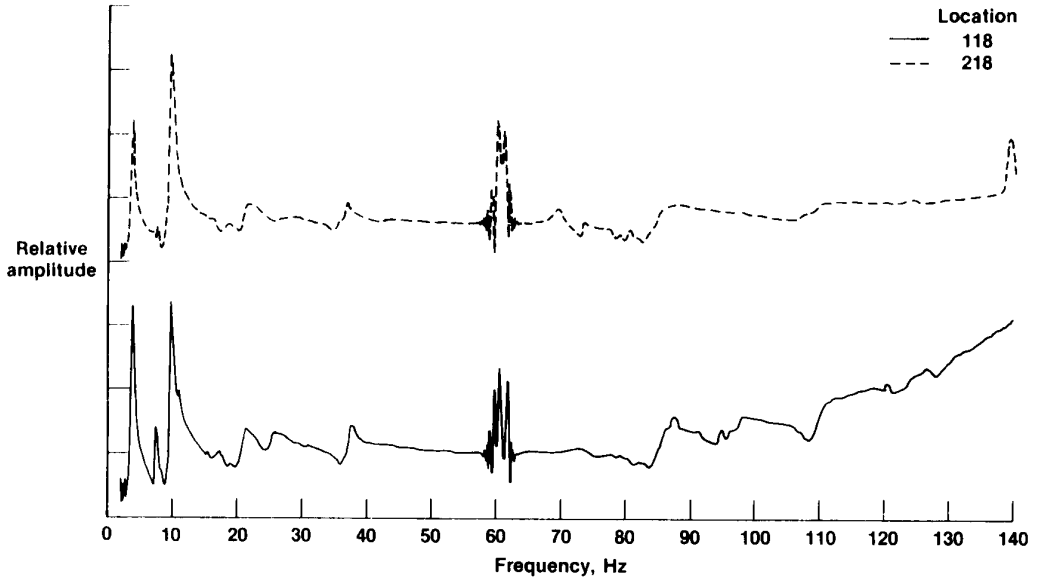

Figure 54. Location 118 and 218 vertical frequency responses due to symmetric sweep at each engine (empty fuel tanks).

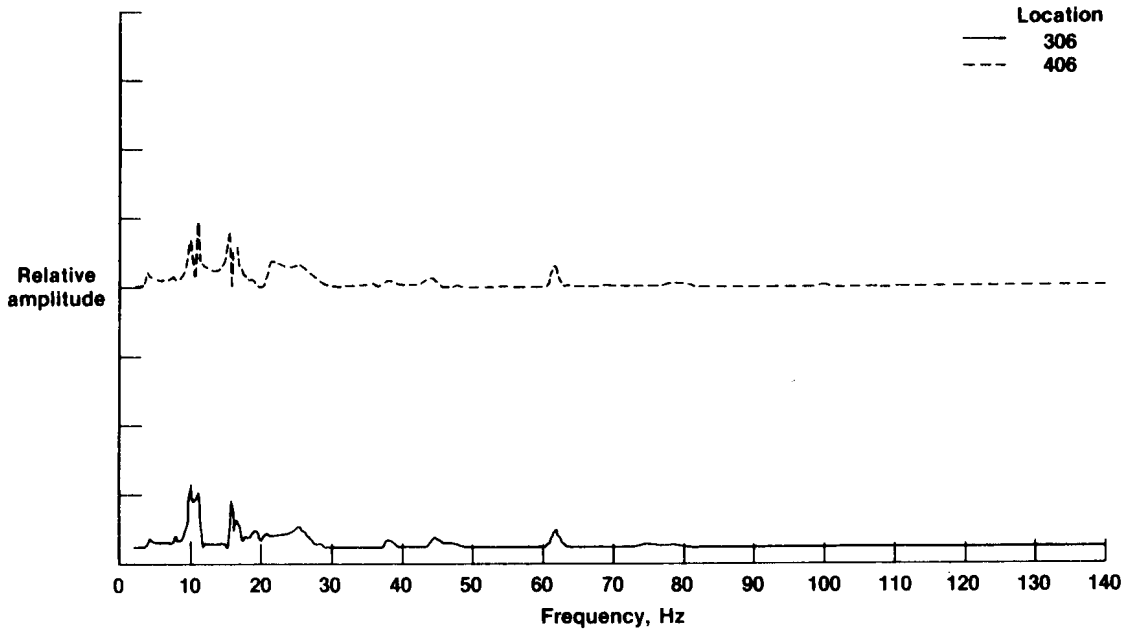

Figure 55. Location 306 and 406 vertical frequency responses due to symmetric sweep at each engine (empty fuel tanks).

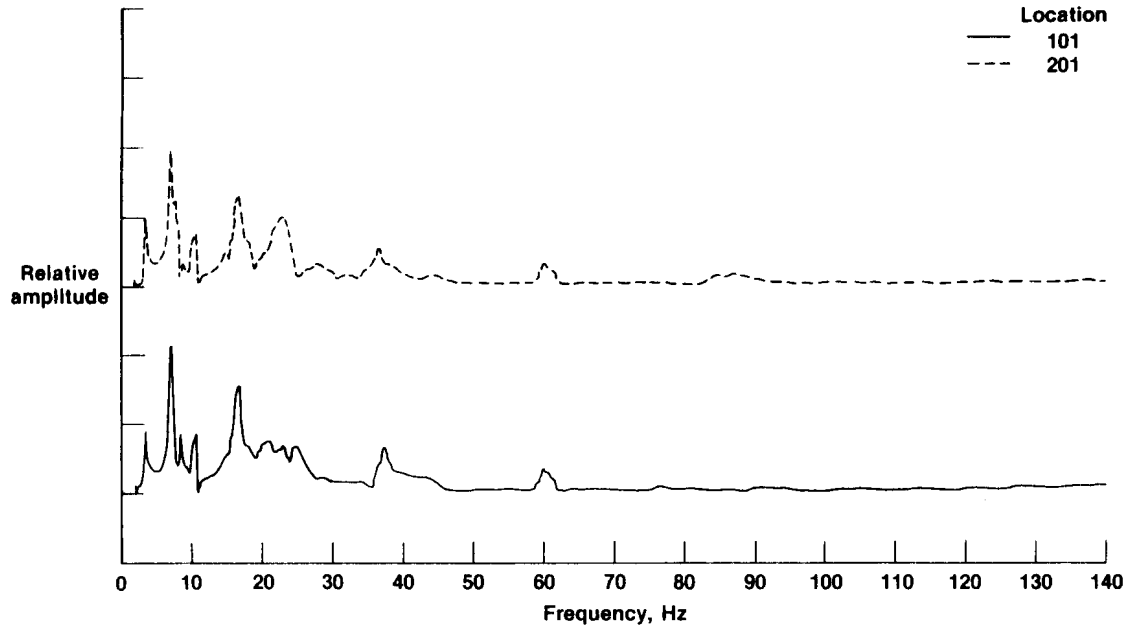

Figure 56. Location 101 and 102 vertical frequency responses due to antisymmetric sweep at each engine (empty fuel tanks).

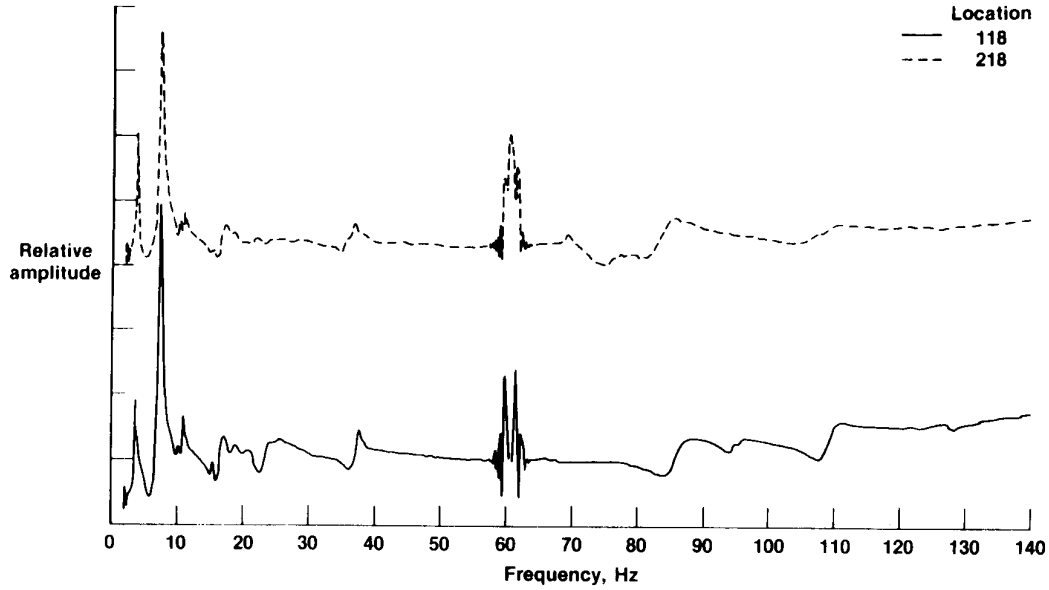

Figure 57. Location 118 and 218 vertical frequency responses due to antisymmetric sweep at each engine (empty fuel tanks).

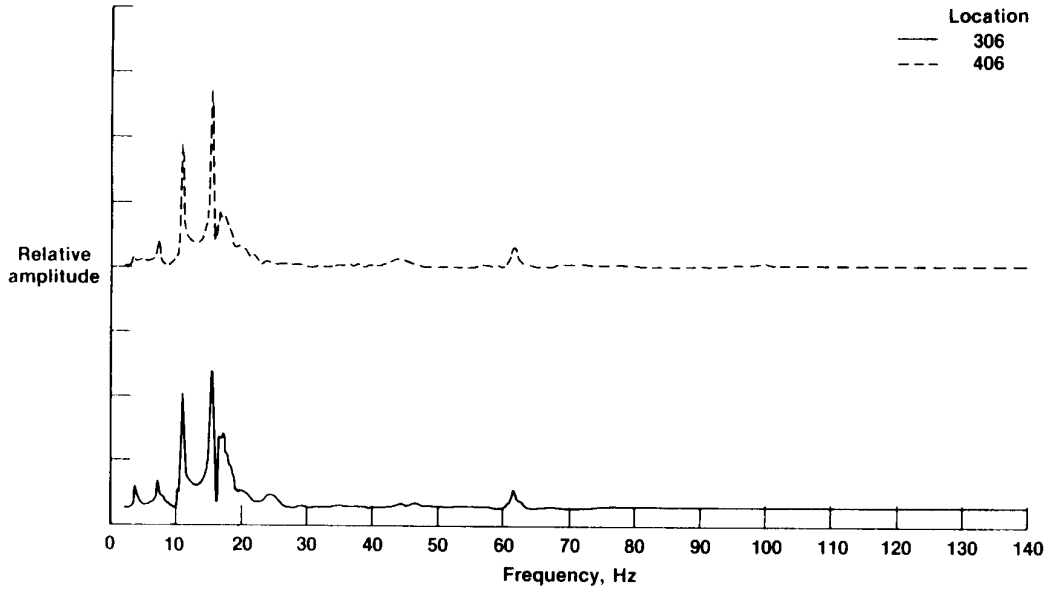

Figure 58. Location 306 and 406 vertical frequency responses due to antisymmetric sweep at each engine (empty fuel tanks).

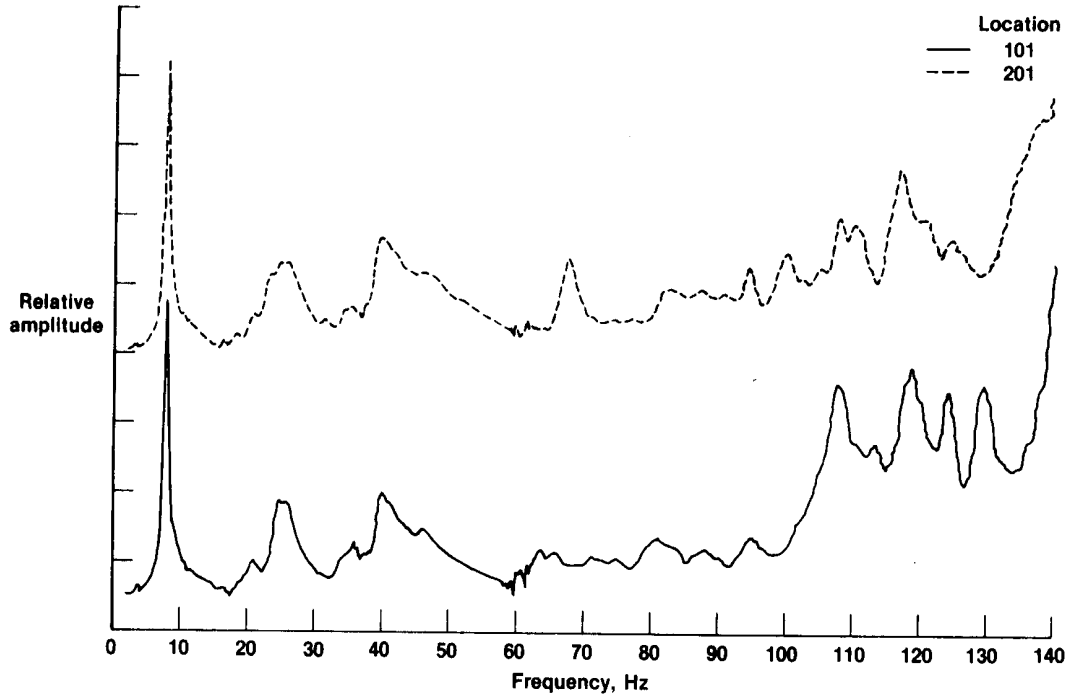

Figure 59. Location 101 and 201 vertical frequency responses due to symmetric sweep at each wingtip (empty fuel tanks).

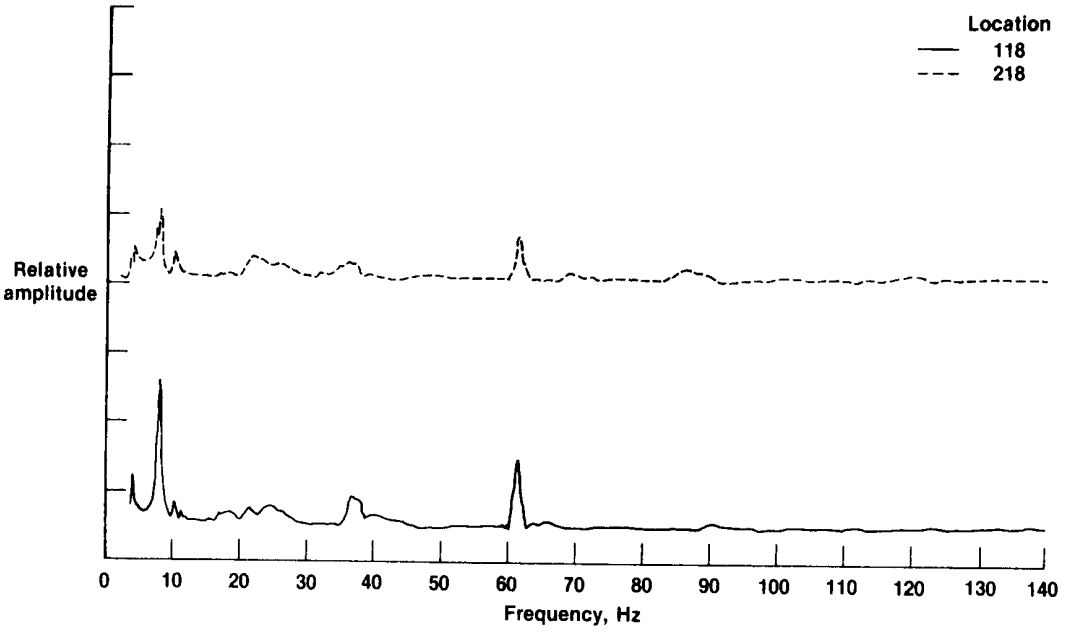

Figure 60. Location 118 and 218 vertical frequency responses due to symmetric sweep at each wingtip (empty fuel tanks).

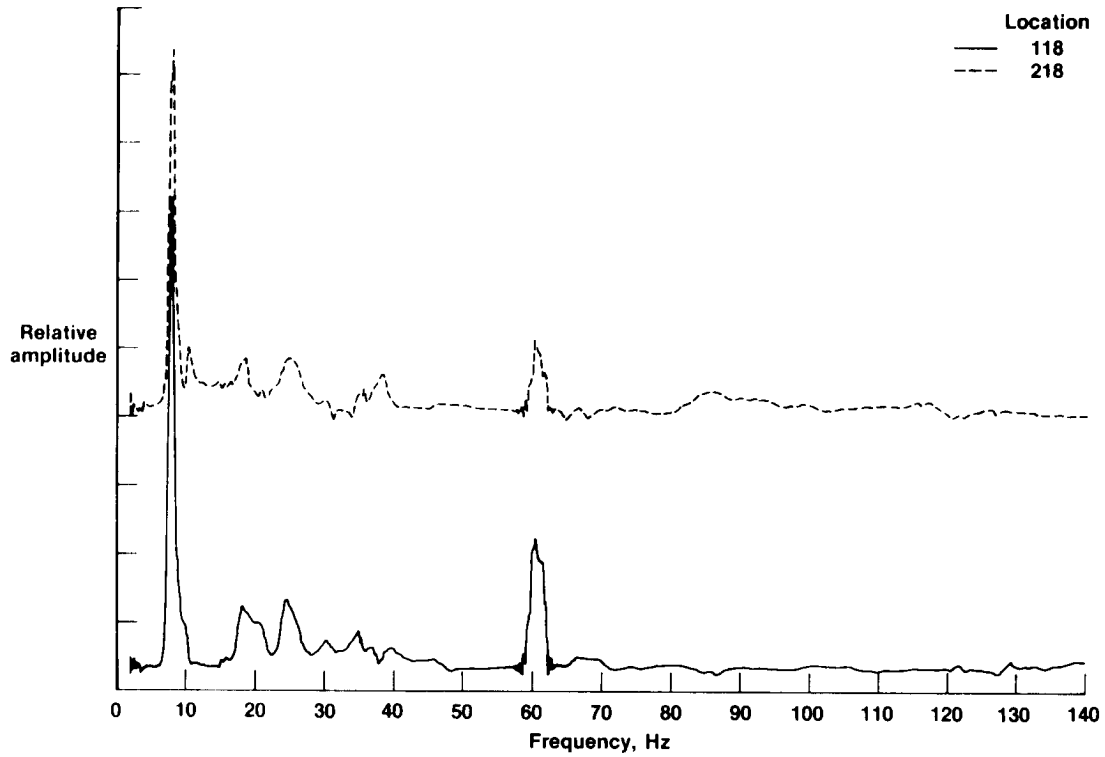

Figure 61. Location 118 and 218 lateral frequency responses due to symmetric sweep at each wingtip (empty fuel tanks).

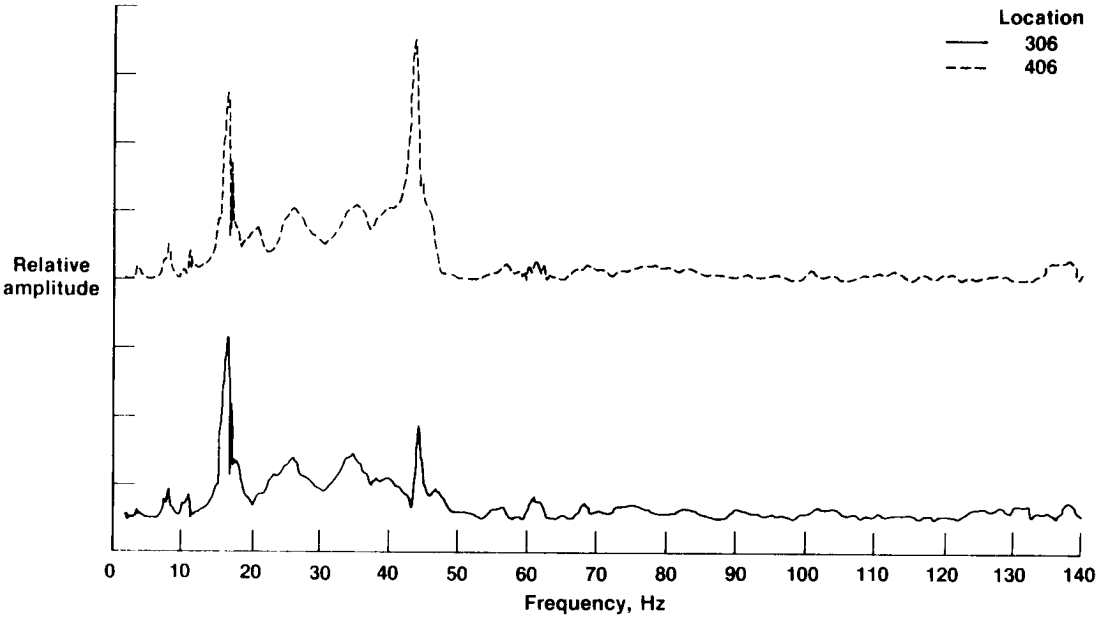

Figure 62. Location 306 and 406 vertical frequency responses due to symmetric sweep at each wingtip (empty fuel tanks).

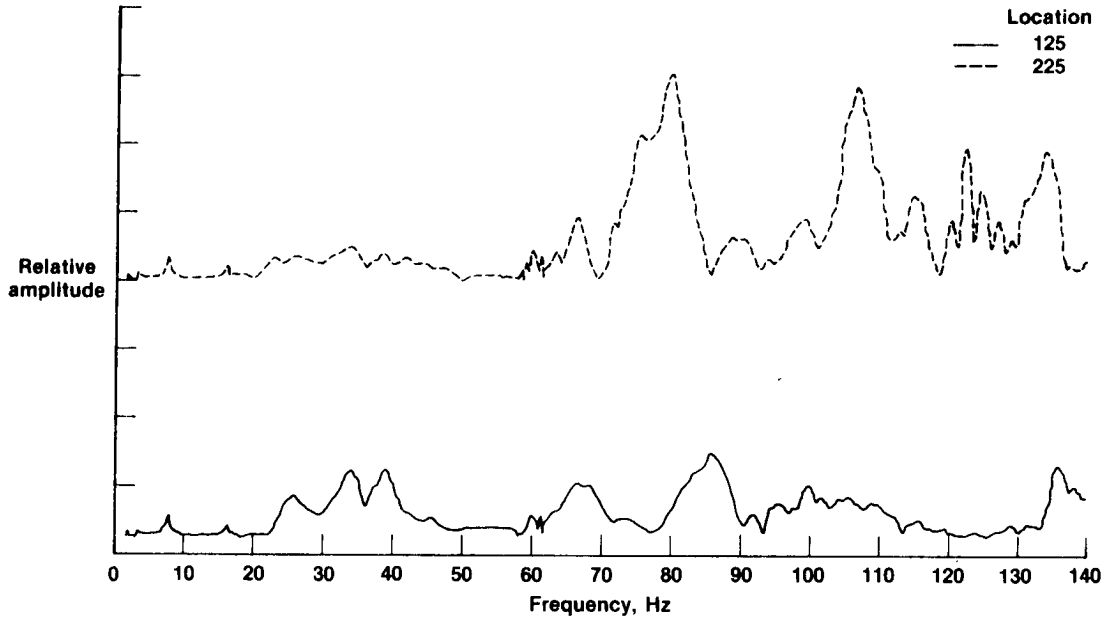

Figure 63. Location 125 and 225 vertical frequency responses due to symmetric sweep at each wingtip (empty fuel tanks).

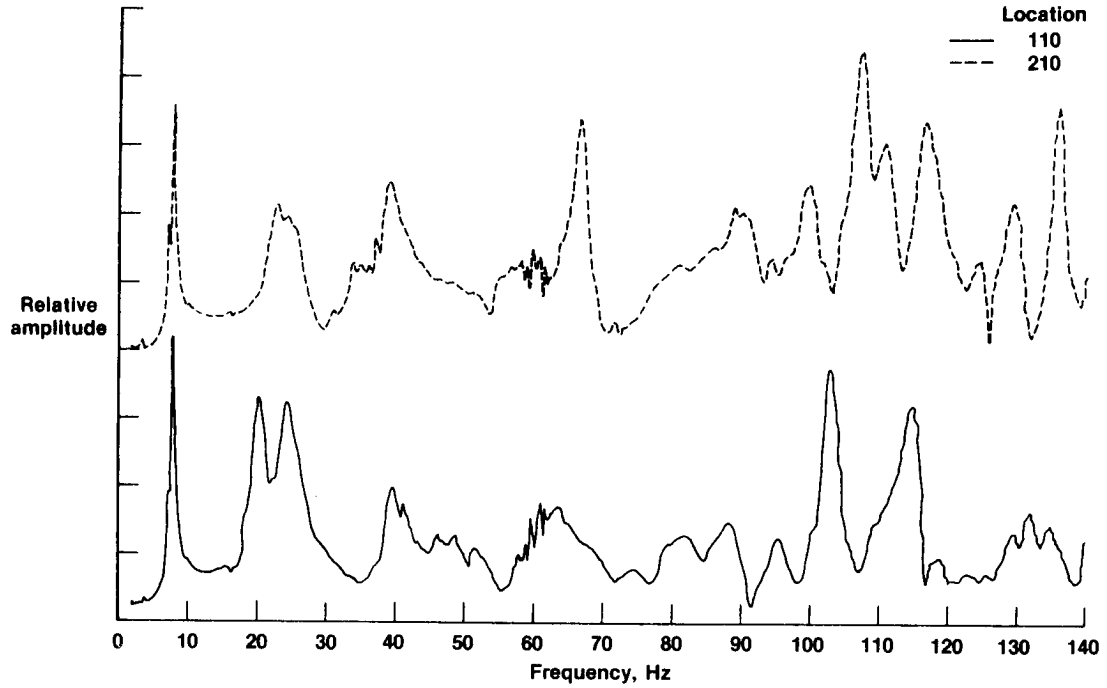

Figure 64. Location 110 and 210 vertical frequency responses due to symmetric sweep at each wingtip (empty fuel tanks).

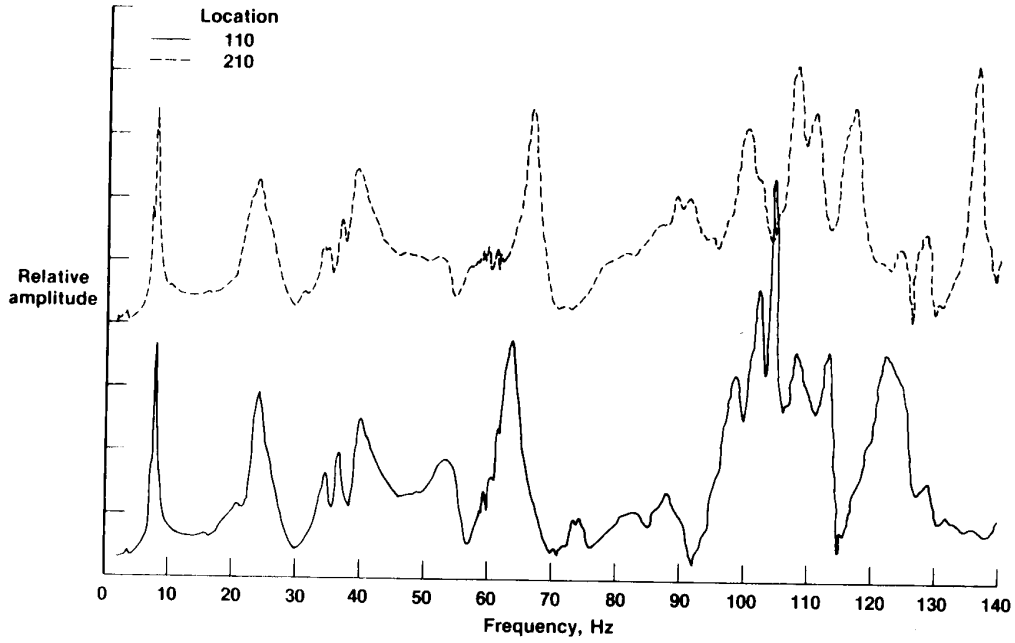

Figure 65. Location 110 and 210 vertical frequency responses (10-lb preload) due to symmetric sweep at each wingtip (empty fuel tanks).

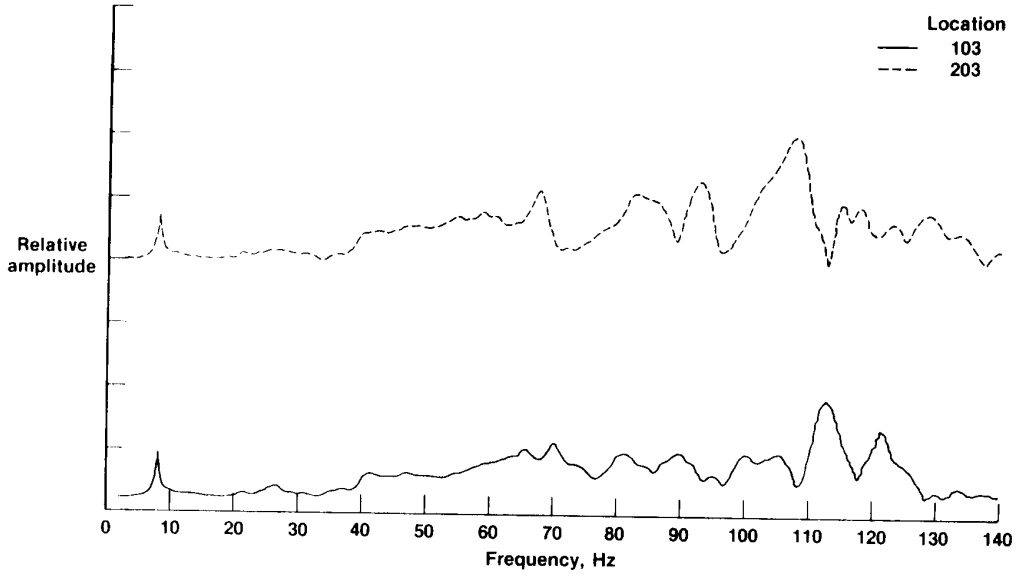

Figure 66. Location 103 and 203 vertical frequency responses due to symmetric sweep at each wingtip (empty fuel tanks).

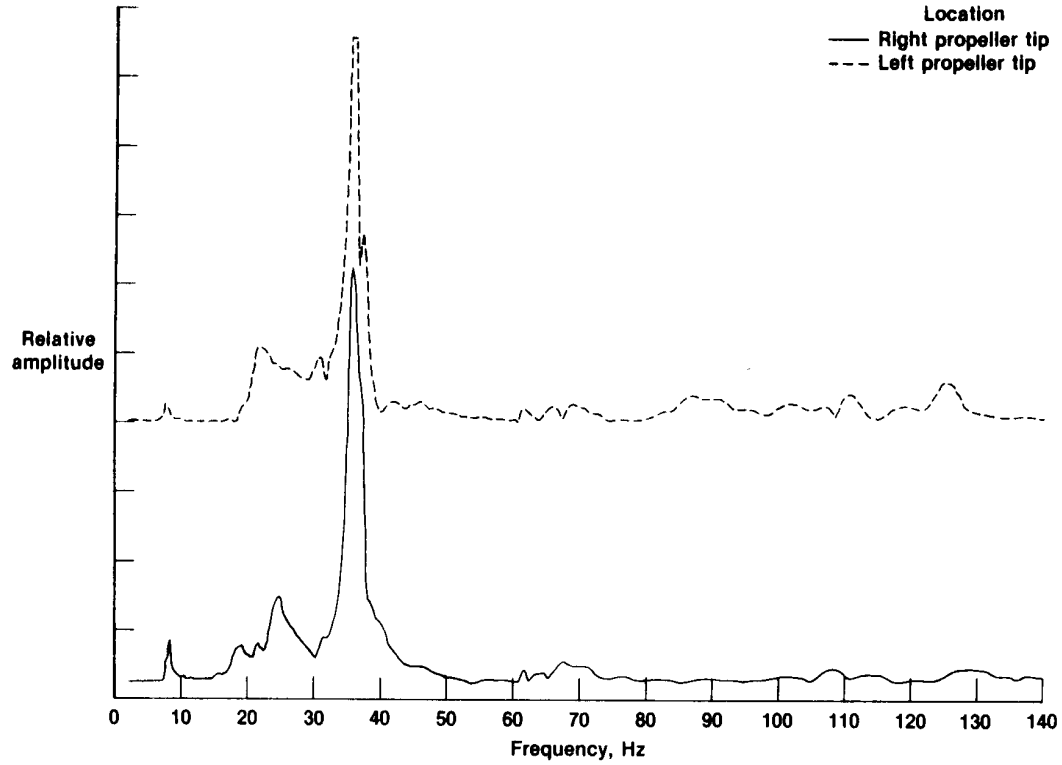

Figure 67. Right and left propeller tip frequency responses due to symmetric sweep at each wingtip (empty fuel tanks).

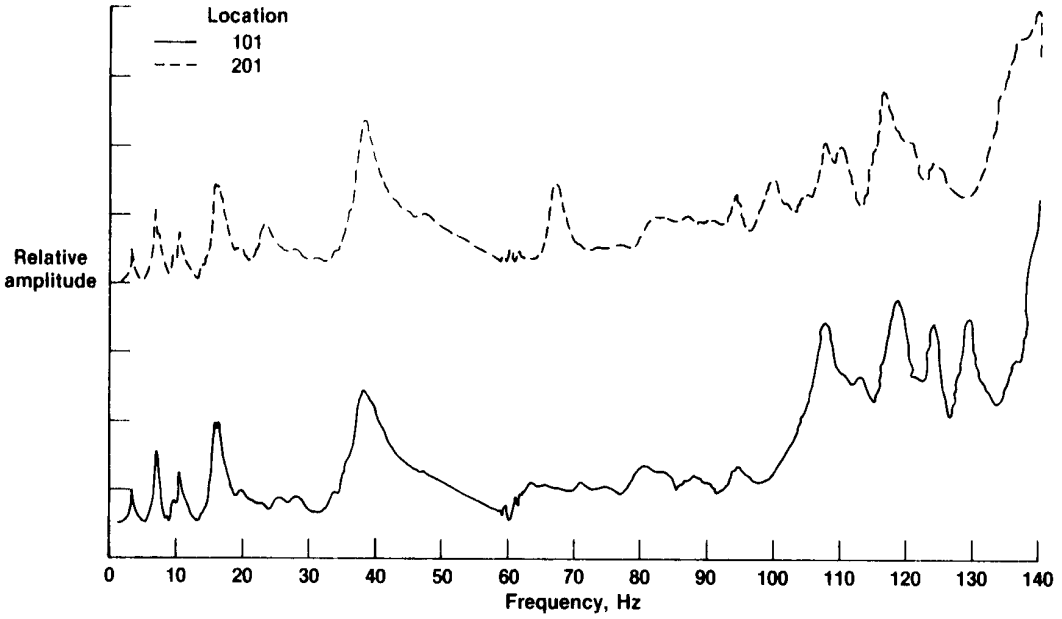

Figure 68. Location 101 and 201 vertical frequency responses due to antisymmetric sweep at each wingtip (empty fuel tanks).

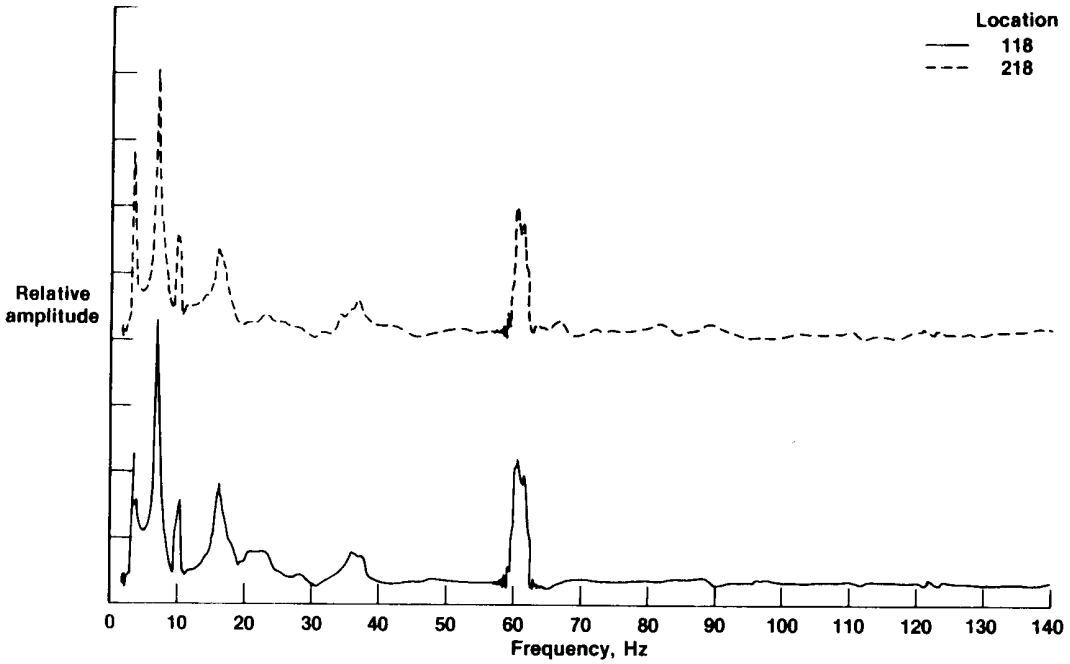

Figure 69. Location 118 and 218 vertical frequency responses due to antisymmetric sweep at each wingtip (empty fuel tanks).

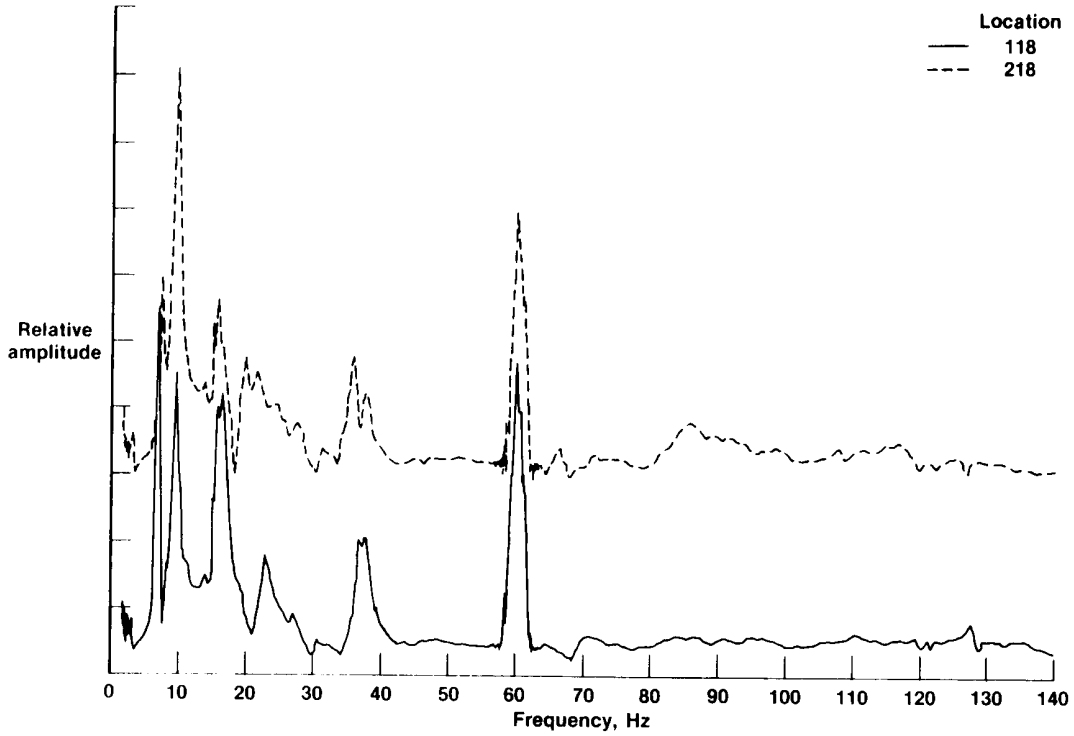

Figure 70. Location 118 and 218 lateral frequency responses due to antisymmetric sweep at each wingtip (empty fuel tanks).

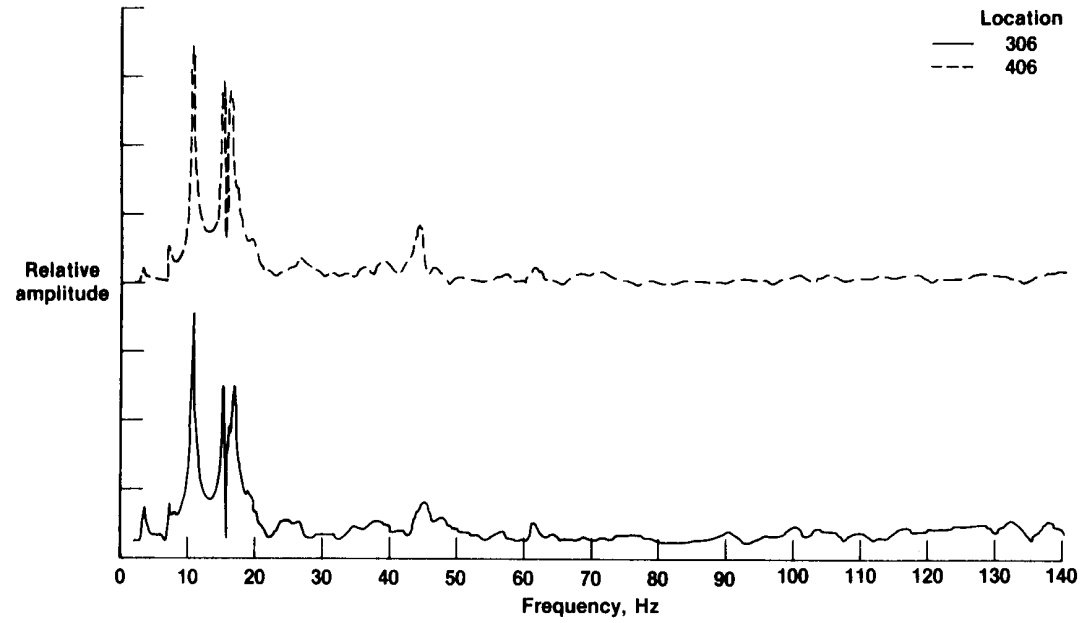

Figure 71. Location 306 and 406 vertical frequency responses due to antisymmetric sweep at each wingtip (empty fuel tanks).

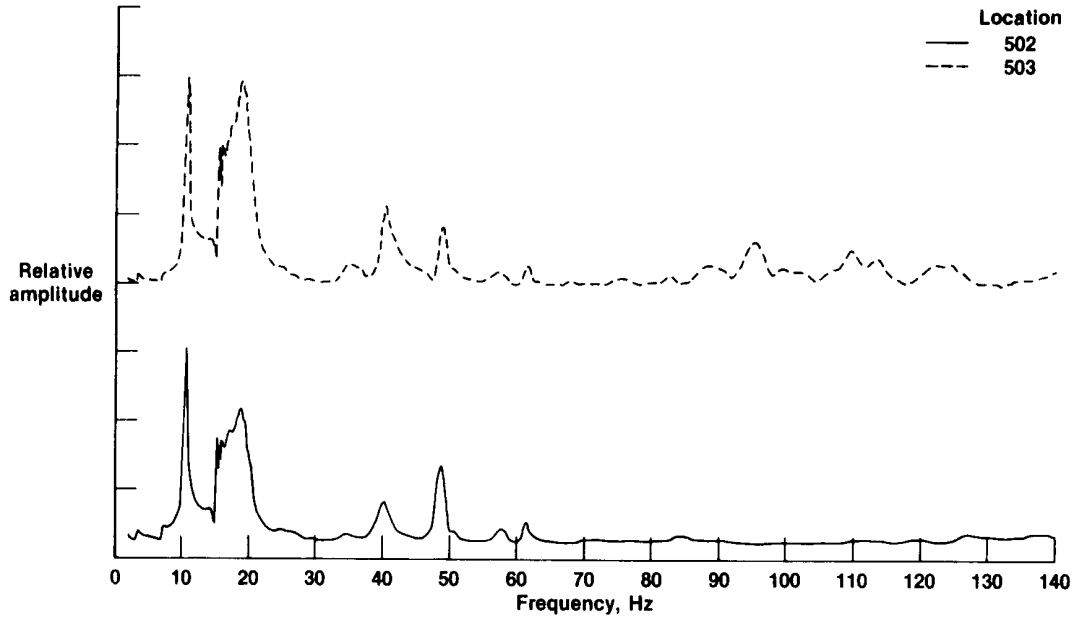

Figure 72. Location 502 and 503 lateral frequency responses due to antisymmetric sweep at each wingtip (empty fuel tanks).

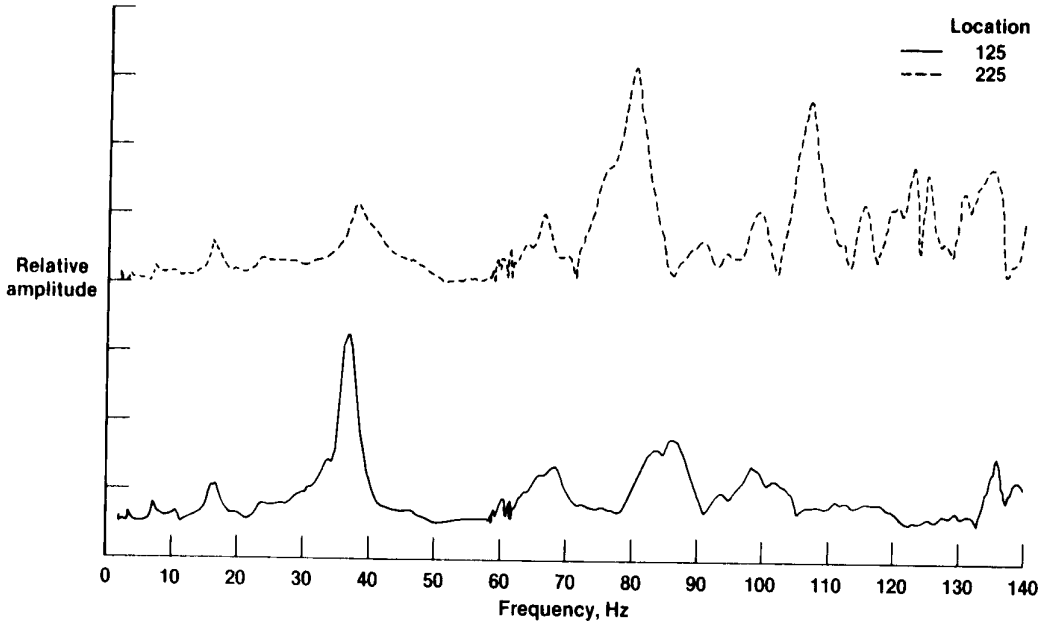

Figure 73. Location 125 and 225 lateral frequency responses due to antisymmetric sweep at each wingtip (empty fuel tanks).

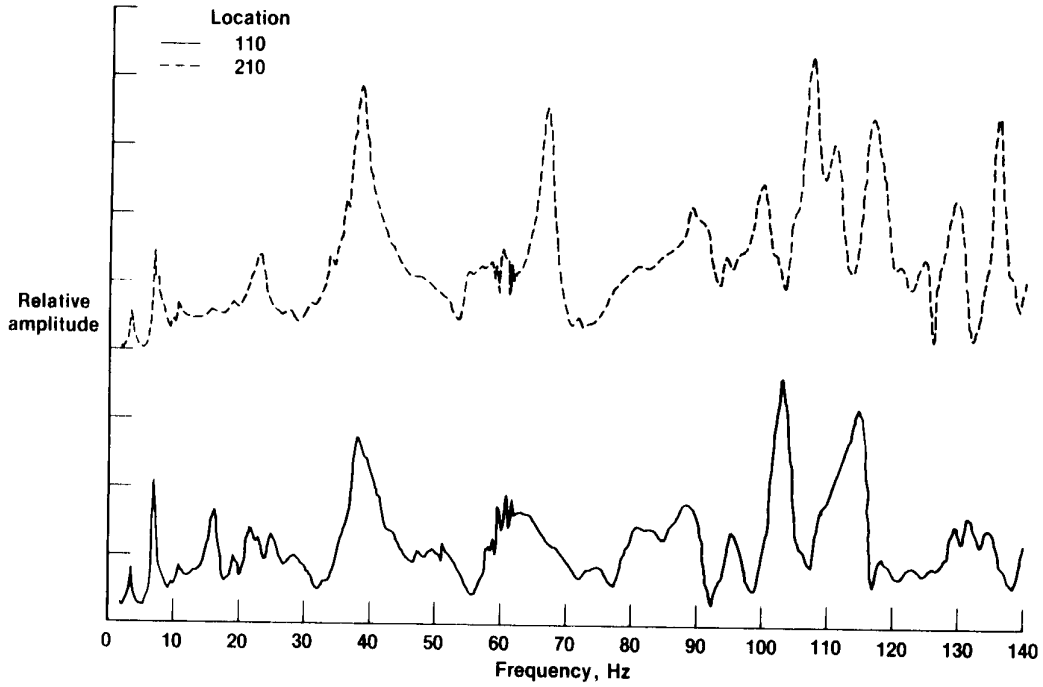

Figure 74. Location 110 and 210 vertical frequency responses due to antisymmetric sweep at each wingtip (empty fuel tanks).

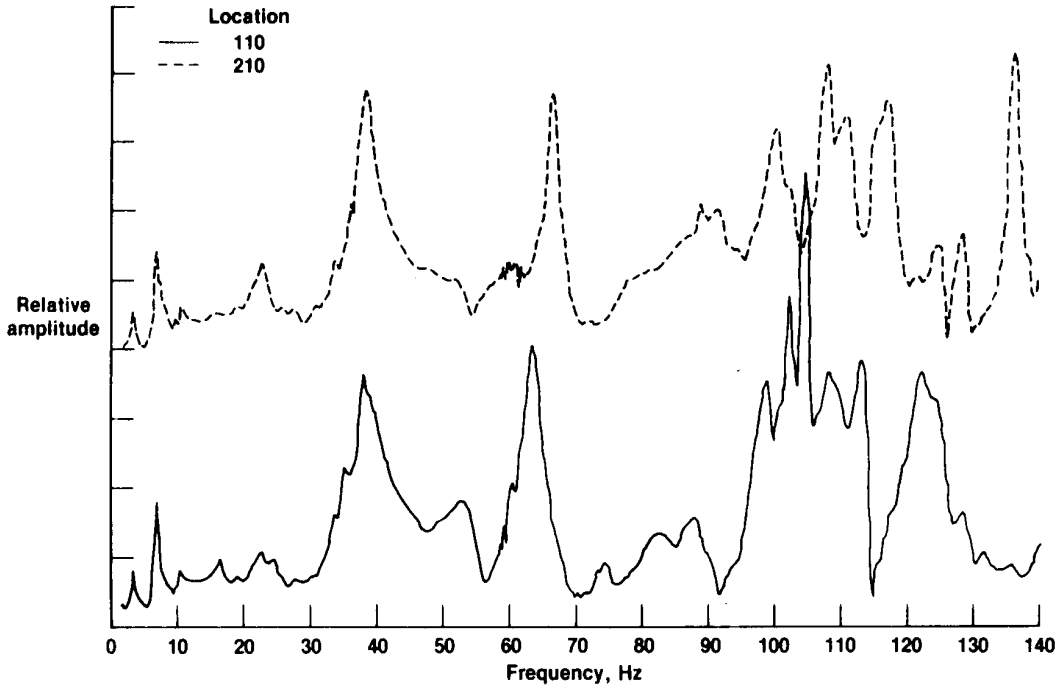

Figure 75. Location 110 and 210 vertical frequency responses (10-lb preload) due to antisymmetric sweep at each wingtip (empty fuel tanks).

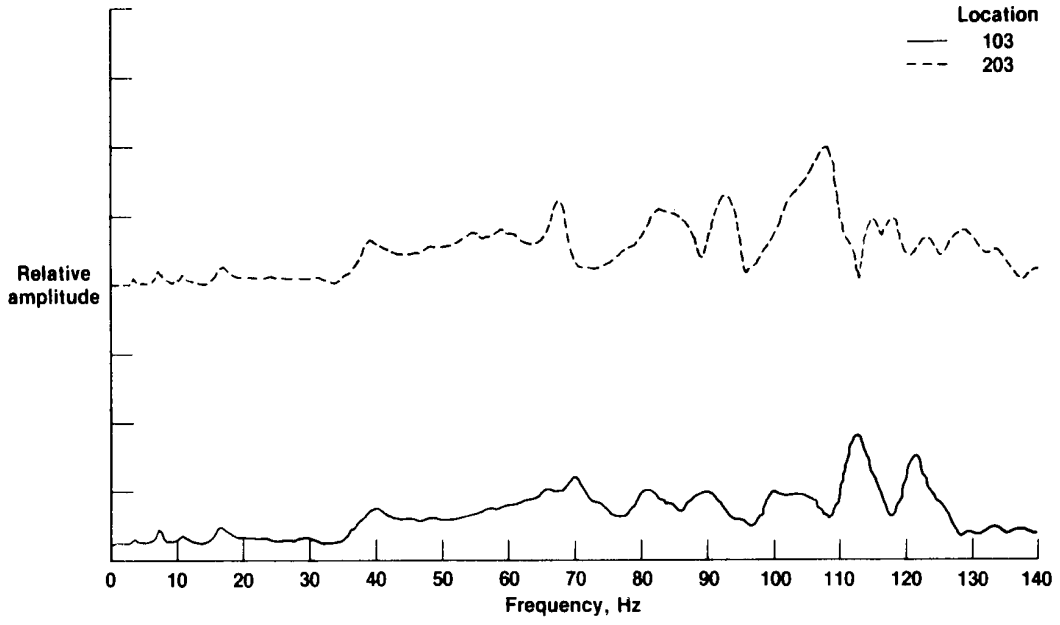

Figure 76. Location 103 and 203 vertical frequency responses due to antisymmetric sweep at each wingtip (empty fuel tanks).

1. Report No.	2. Government Accession No.	3. Recipient's Catalog No.
NASA TM-86741		

4. Title and Subtitle	5. Report Date
Modified U.S. Army U-8F Ground Vibration Test	August 1986
	6. Performing Organization Code

7. Author(s)	8. Performing Organization Report No.
Michael W. Kehoe	H-1297
	10. Work Unit No.
	RTOP 505-63-21

9. Performing Organization Name and Address	11. Contract or Grant No.
NASA Ames Research Center Dryden Flight Research Facility P.O. Box 273 Edwards, CA 93523-5000	
	13. Type of Report and Period Covered
12. Sponsoring Agency Name and Address	Technical Memorandum
National Aeronautics and Space Administration Washington, D.C. 20546	14. Sponsoring Agency Code

15. Supplementary Notes

16. Abstract

The Dryden Flight Research Facility of NASA Ames Research Center conducted a ground vibration test on a modified U.S. Army U-8F airplane. Modifications included new engines, propellers, and engine-mount truss assemblies. The ground vibration test was conducted using sine dwell, single-point random, and impact excitations. The test was performed to determine modal frequencies, mode shapes, and structural damping coefficients of the airframe and propeller with full and empty fuel tanks. The data presented include frequency response plots, rigid-body and structural modal frequencies, and mode shapes.

17. Key Words (Suggested by Author(s))	18. Distribution Statement
U-8F airplane Ground vibration test Modal analysis	Unclassified – Unlimited STAR category 05

19. Security Classif. (of this report)	20. Security Classif. (of this page)	21. No. of Pages	22. Price*
Unclassified	Unclassified	48	A03

For sale by the National Technical Information Service, Springfield, Virginia 22161.